

---

# MLDGG: META-LEARNING FOR DOMAIN GENERALIZATION ON GRAPHS

---

Qin Tian<sup>1</sup>, Chen Zhao<sup>2</sup>, Minglai Shao<sup>3</sup>, Wenjun Wang<sup>1</sup>, Yujie Lin<sup>3</sup>, Dong Li<sup>2</sup>

<sup>1</sup>College of Intelligence and Computing, Tianjin University

<sup>2</sup>Department of Computer Science, Baylor University

<sup>3</sup>School of New Media and Communication, Tianjin University

{tianqin123,shaoml,linyujie\_22}@tju.edu.cn, {chen\_zhao,dong\_li1}@baylor.edu

## ABSTRACT

Domain generalization on graphs aims to develop models with robust generalization capabilities, ensuring effective performance on the testing set despite disparities between testing and training distributions. However, existing methods often rely on static encoders directly applied to the target domain, constraining its flexible adaptability. In contrast to conventional methodologies, which concentrate on developing specific generalized models, our framework, MLDGG, endeavors to achieve adaptable generalization across diverse domains by integrating cross-multi-domain meta-learning with structure learning and semantic identification. Initially, it introduces a generalized structure learner to mitigate the adverse effects of task-unrelated edges, enhancing the comprehensiveness of representations learned by Graph Neural Networks (GNNs) while capturing shared structural information across domains. Subsequently, a representation learner is designed to disentangle domain-invariant semantic and domain-specific variation information in node embedding by leveraging causal reasoning for semantic identification, further enhancing generalization. In the context of meta-learning, meta-parameters for both learners are optimized to facilitate knowledge transfer and enable effective adaptation to graphs through fine-tuning within the target domains, where target graphs are inaccessible during training. Our empirical results demonstrate that MLDGG surpasses baseline methods, showcasing the effectiveness in three different distribution shift settings.

**Keywords** Domain Generalization, Graph Learning, Meta Learning

## 1 Introduction

Domain generalization is a fundamental research area in machine learning that aims to enhance the ability of models learned from source domains to generalize well to different target domains [1, 2, 3, 4, 5, 6, 7, 8, 9, 10, 11, 12]. While handling distribution shifts across domains on Euclidean data has achieved significant success [13, 14], there has been limited focus on graph-structured data due to specific challenges where domains are characterized by variations of node features and graph topological structures simultaneously. Fig. 1 illustrates the presence of distribution disparities on graphs, with each graph sampled from a distinct domain. Consequently, a model trained on one graph domain (*e.g.*, gamer networks, TWITCH) may exhibit poor generalization performance when deployed in a different domain (*e.g.*, social networks, FB-100).

To address the problem of domain generalization on graphs, several efforts have been made. Existing approaches on invariant learning with Graph Neural Networks (GNNs) [15, 16] focus on encoding invariant information of graphs by minimizing the risk across various environments under the assumption that the information determining labels remain constant. They usually assume access to abundant and diverse training domains, prompting researchers to propose data augmentation [17, 18, 19] to alleviate the problem, which strives to diversify the training domains as much as possible to improve the generalization ability of the model. However, an overly flexible domain augmentation strategy can create implausible augmented domains [20]. Additionally, the complexity of real-world graph structures and the

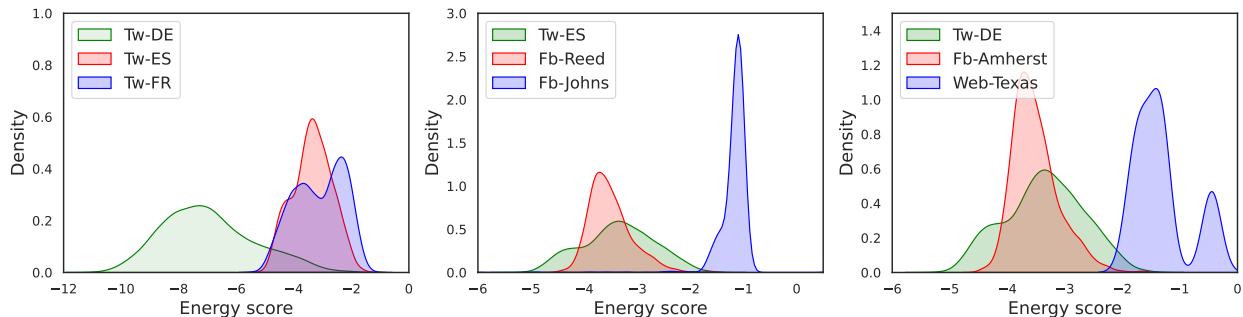


Figure 1: Visualizations of distribution shifts on graphs demonstrated using energy scores [24] of nodes across different graphs, where each graph is sampled from a distinct domain characterized by variations of node features and topological structures simultaneously. The legend of all sub-figures follows the same naming format, *i.e.*, "DataName - DomainName". (Left) Graphs are sampled from the same dataset TWITCH [25]. (Middle and Right) Graphs are sampled from different datasets, TWITCH, FB-100 [26], and WEBKB [27].

often unknown underlying data generation mechanisms make it challenging to acquire the knowledge necessary for generating new graphs.

Moreover, to alleviate the above obstacles and enhance the interpretability of generalized models, causal reasoning is often combined with invariant learning [21, 22]. The invariance principle from causality elucidates and models the underlying generative processes of graphs, targeting the identification of stable causal relationships across different domains. Nevertheless, studies show that trained GNNs are heavily biased towards specific graph structures and cannot effectively address the domain variations on graph topology structures [23].

Additionally, some studies integrate structure learning to improve the robustness of generalized GNNs, such as capturing the domain-independent and domain-invariant clusters to learn invariant representations [23] by training static encoders shared by all source graphs [28]. However, capturing invariant topology structure learners across domains reduces the adaptability of the structural encoder and limits its ability to accommodate various distributions. Hence, it is urgent to train models who possess transferable knowledge across domains with various distribution shifts.

In this paper, we propose a novel cross-multi-domain meta-learning framework, MLDGG, designed to acquire transferable knowledge from graphs sampled in the source domain and generalize to those in the target domain, where target graphs are inaccessible during training. Specifically, to address the problem of node-level domain generalization on graphs, where domain variations are characterized by graph topological structures and node features, MLDGG comprises two key components: a structure learner and a representation learner. The structure learner aims to mitigate the adverse effects of task-unrelated edges and capture structure knowledge shared across different domains, enhancing the comprehensiveness of representations learned by GNNs. The representation learner disentangles semantic and variation factors to capture the invariant patterns of the truly predicting properties in different domains. In the context of meta-learning, the goal of MLDGG aims to learn optimal meta-parameters (initialization) for both learners so that they can facilitate knowledge transfer and enable effective adaptation to graphs through fine-tuning within the target domains. Our contributions are summarized as follows:

- We propose a novel cross-multi-domain meta-learning framework on graphs. It is designed to acquire transferable knowledge from graphs sampled in the source domain and generalize to those in the target domain, where target graphs are inaccessible during training.
- The framework consists of two key learners: a structure learner, which captures shared topology patterns across different graph domains to enhance the robustness of GNNs, and a representation learner, which disentangles domain-invariant semantics from domain-specific variations. In the context of meta-learning, the parameter initializations for both learners are optimized to facilitate knowledge transfer and enable effective adaptation to graphs through fine-tuning within the target domains.
- Empirically, we conduct three distinct cross-domain settings to assess the generalization ability of MLDGG for node-level prediction tasks under different degrees of distribution shifts using real-world graph datasets. Our method consistently outperforms state-of-the-art baseline approaches.

## 2 Related Work

**Domain Generalization on Graphs.** Domain generalization aims to generalize a model trained on multiple seen domains with diverse distributions to perform well on an unseen target domain [29]. The study of domain generalization on graphs presents significant challenges due to the irregular nature of graph data and the complex dependencies between nodes [30, 31]. Methodologically, various strategies such as robust optimization [32, 33], invariant learning [34, 16, 15], causal approaches [21, 22] and meta-learning domain generalization [35, 36, 37, 38] have been employed to tackle this problem. Robust optimization improves the generalization ability by improving the model’s performance in the worst-case data distribution. Invariant learning minimizes prediction variance across domains to capture invariant features across domains. Causal approaches are dedicated to separating inclusive information factors (semantic information) and irrelevant factors, utilizing the principles of causal graphs in an unsupervised or semi-supervised manner. In addition, GraphGlow [28] improves GNN generalization by learning generic graph structures. It trains a static structure encoder to capture invariant structure information across domains and apply it in the target domain, which reduces the adaptability of the structural encoder and limits its ability to accommodate various distributions. Despite GNNs’ ability to extract abstract representations, they mix the domain-invariant semantic factor with the domain-specific variation factor. Meta-learning learns prior experiences during meta-training and transforms learned knowledge to the target domain by simple fine-tuning. Following similar spirits, we use a combination of learning domain-invariant semantic information and learning-to-learn strategies to achieve domain generalization across domains.

**Meta-Learning on Graphs.** Meta-learning, also known as "learning to learn", focuses on the ability of a model to learn and adapt to new tasks or domains quickly and efficiently [39, 40]. It has been widely used in generalization problems [41, 42, 43, 20]. Consequently, meta-learning for graphs generally combines the advantages of GNNs and meta-learning to implement generalization on irregular graph data [44, 45]. From the learning tasks of view, these methods generally fall into three categories, node-level [46, 47], edge-level [44, 38] and graph-level [48, 49]. Methodologically, these approaches incorporate metric-based [50, 51], which are aimed at learning metrics to quantify the similarity between task-specific support and query sets, and optimization-based methods [52, 53] that concentrate on effectively training a well-initialized learner capable of rapidly adapting to new few-shot tasks via simple fine-tuning. However, they only consider the scene where all tasks originate from the same domain, the challenge of generalizing prior experiences from cross-multi-domain graphs during meta-training and transferring knowledge to unseen domains is unexplored in the existing literature.

## 3 Preliminaries

We list all notations used in this paper in Table 7 in Appendix A.

**Node-level Domain Generalization on Graphs.** Given a set of graphs  $\mathcal{G} = \{G^{e_i}\}_{i=1}^{|\mathcal{E}|}$ , where each graph  $G^{e_i} = (A^{e_i}, X^{e_i})$  is sampled from a unique domain  $e_i \in \mathcal{E}$  and a domain  $e_i$  is defined as a joint distribution  $\mathbb{P}(A^{e_i}, X^{e_i})$ . In each graph  $G^{e_i}$ , we denote  $A^{e_i} \in \{0, 1\}^{|\mathcal{V}^{e_i}| \times |\mathcal{V}^{e_i}|}$  the adjacency matrix, where  $\mathcal{V}^{e_i}$  is a collection of nodes.  $X^{e_i} = \{\mathbf{x}_j^{e_i}\}_{j=1}^{|\mathcal{V}^{e_i}|} \in \mathbb{R}^{|\mathcal{V}^{e_i}| \times D^{e_i}}$  represents the node feature matrix of  $D$ -dimensional vectors.  $\mathbf{y}^{e_i} = \{y_j^{e_i}\}_{j=1}^{|\mathcal{V}^{e_i}|} \in \mathbb{R}^{|\mathcal{V}^{e_i}|}$  denotes node labels in  $G^{e_i}$ .

For node-level domain generalization, each graph  $G^{e_i} \in \mathcal{G}$  is associated with a specific variation in graphic topology  $A^{e_i}$  and node features  $X^{e_i}$ . The graph set  $\mathcal{G}$  is partitioned into multiple source graphs  $\mathcal{G}_s = \{G^{e_i}\}_{i=1}^K$  where  $K = |\mathcal{E}_s|$  and  $\mathcal{E}_s \subset \mathcal{E}$ , and target graphs  $\mathcal{G}_t$  with  $\mathcal{E}_t = \mathcal{E} \setminus \mathcal{E}_s$ . The objective is to maintain satisfactory generalization performance in node-level prediction accuracy transitioning from given source graphs  $\mathcal{G}_s$  to target graphs  $\mathcal{G}_t$ , with the condition that  $\mathcal{G}_t$  remains inaccessible during training.

**Meta-Learning** is an approach aimed at training a model over a range of tasks to be able to adapt to new tasks rapidly [54, 55, 20], where each task  $\mathcal{T}^i \sim \mathbb{P}(\mathcal{T})$  associated with a data batch is partitioned into a support set  $\mathcal{T}_{sup}^i$  for the learning phase and a query set  $\mathcal{T}_{qry}^i$  for evaluation purposes. Meta-learning can be described as "learning to learn" because it involves finding a meta-parameter  $\theta$  from which one can quickly derive multiple optimized parameters  $\{\theta^i\}_{i=1}^M$  specific to individual tasks  $\{\mathcal{T}^i\}_{i=1}^M$ .

Model-agnostic meta-learning (MAML) [39] is a notable gradient-based meta-learning approach that has demonstrated remarkable success in generalization. The core assumption of MAML is that some internal representations are better suited to transfer learning.

During training, the model first learns from  $\mathcal{T}_{sup}^i$  for each task  $\mathcal{T}^i$  and accordingly optimizes the task-specific parameter to  $\theta^i$  with one or few gradient steps. The meta-parameter  $\theta$  is updated through query losses evaluated from  $\{\mathcal{T}_{qry}^i\}_{i=1}^M$

based on  $\{\theta^i\}_{i=1}^M$ .

$$\theta = \arg \min_{\theta} \frac{1}{M} \sum_i \ell(\theta^i, \mathcal{T}_{qry}^i), \text{ where } \theta^i = \theta - \alpha \nabla \ell(\theta, \mathcal{T}_{sup}^i), \quad (1)$$

where  $\ell : \Theta \times \mathbb{R}^d \rightarrow \mathbb{R}$  is the cross-entropy loss for classification and  $\alpha > 0$  is the learning rate. The goal of MAML is to learn an effective model initialization  $\theta$  using  $M$  training tasks, enabling rapid fine-tuning on the support set  $\mathcal{T}_{sup}^t$  of the target task  $\mathcal{T}^t$  to achieve optimal performance on  $\mathcal{T}_{qry}^t$ , where  $\mathcal{T}^t = \{\mathcal{T}_{sup}^t, \mathcal{T}_{qry}^t\}$ .

Graph generalization using MAML leverages a similar GNN-based task distribution to accumulate transferable knowledge from prior learning experiences. However, the original MAML [39] assumes that all tasks originate from the same distribution, which hinders its ability to generalize across multiple domains [56, 57]. Additionally, GNNs can introduce noise information from task-unrelated edges, negatively impacting performance. As discussed in Section 1, GNN methods combined with structural optimization typically learn a static structure, which constrains the model’s ability to generalize to varying topology distribution shifts. To overcome these limitations, a cross-multi-domain robust algorithm is required, as we will discuss next.

**Problem Setup.** To address the problem of node-level domain generalization on graphs, where each domain is characterized by variations on both topology structures and node attributes, learning cross-multi-domain shared graph topology and node representation information is essential for capturing transferable knowledge across different domains. As shown in Fig. 2, a novel framework MLDGG is proposed in the context of meta-learning with two key components: a structure learner  $f_t : \Theta \times (\mathcal{A} \times \mathcal{X}) \rightarrow \mathcal{A}$  parameterized by  $\theta_t$  and a representation learner  $f_r : \Theta \times \mathbb{R}^d \rightarrow \mathbb{R}^d$  parameterized by  $\theta_r$ . The goal of MLDGG aims to learn a good parameter initialization  $\theta = \{\theta_t, \theta_r\}$  across all given source graphs  $\{G^{e_i}\}_{i=1}^K, \forall e_i \in \mathcal{E}_s$ , such that the learned  $\theta$  can be effectively adapted to the target graph  $G^{e_T}, e_T \in \mathcal{E}_t$ , which is inaccessible during training.

$$\theta = \arg \min_{\theta} \frac{1}{M} \sum_{i=1}^M \ell(\theta^{e_i}, \mathcal{T}_{qry}^{e_i}), \quad \forall e_i \in \mathcal{E}_s \quad (2)$$

$$\text{where } \theta^{e_i} = \theta - \alpha \nabla \ell(\theta, \mathcal{T}_{sup}^{e_i}),$$

$$\mathcal{T}_{sup}^{e_i} = E_s \left( \theta_s, \text{GNN}(\theta_g^{e_i}, G^{e_i}) \oplus \text{GNN}(\theta_g^{e_i}, G^{e_i} = (X^{e_i}, f_t(\theta_t, G^{e_i}))) \right),$$

where  $M \leq K$  represents the number of tasks and  $\oplus$  is denoted as element-wise addition operation.  $\text{GNN} : \Theta \times (\mathcal{A} \times \mathcal{X}) \rightarrow \mathbb{R}^d$  is a graphic representation function, parameterized by  $\theta_g^{e_i}$  specific to the domain  $e_i$ . The representation learner  $f_r$  consists of a semantic encoder  $E_s : \Theta \times \mathbb{R}^d \rightarrow \mathbb{R}^s$ , a variation encoder  $E_v : \Theta \times \mathbb{R}^d \rightarrow \mathbb{R}^v$ , and a decoder  $D : \Theta \times \mathbb{R}^{s+v} \rightarrow \mathbb{R}^d$ . We thus denote  $\theta_r$  as consisting of the parameters  $\theta_s, \theta_v$ , and  $\theta_d$ , respectively, *i.e.*,  $\theta_r = \{\theta_s, \theta_v, \theta_d\}$ . Detailed setting and training of  $f_r$  is introduced in Section 4.2.  $\mathcal{T}_{sup}^{e_i}$  and  $\mathcal{T}_{qry}^{e_i}$  are support and query sets of the domain  $e_i$ , which are randomly sampled from the output of the semantic encoder  $E_s$ . Inspired by MAML, meta-parameters  $\theta = \{\theta_t, \theta_r\}$  and task-specific parameters  $\theta^{e_i} = \{\theta_t^{e_i}, \theta_r^{e_i}\}$  are updated interchangeably through the bi-level optimization, using query sets  $\{\mathcal{T}_{qry}^{e_i}\}_{i=1}^M$  and support sets  $\{\mathcal{T}_{sup}^{e_i}\}_{i=1}^M$ , respectively. The learned  $\theta$  is further fine-tuned to  $\theta^{e_T}$  using  $\mathcal{T}_{sup}^{e_T}$  from the target domain. The generation performance is then evaluated on  $\theta^{e_T}$  using  $\mathcal{T}_{qry}^{e_T}$ .

## 4 Methodology

The primary challenges of MLDGG involve modeling and capturing generalizable structure patterns across multiple domains, as well as disentangling domain-invariant semantic factors and domain-specific variation factors. To this end, the structure learner  $f_t$  is devoted to capturing shared structural information across domains while enhancing the comprehensiveness of representations learned by GNN through mitigating the adverse effects of task-unrelated edges (Sec. 4.1). Additionally, the representation learner  $f_r$  captures the invariant patterns of the truly predictive properties through the semantic encoder  $E_s$  by disentangling semantic and variation factors in node representations based on the causal invariance principle (Sec. 4.2). Finally, in Sec. 4.3, we integrate two learners within the meta-learning framework to capture transferable knowledge across various domains. For simplicity, in this section, domain  $e_i$  is simplified to  $i$ .

### 4.1 Structure Learner

For graph data with both attributes and topologies, how to learn as comprehensive and rich node representation as possible is a problem that has been explored. One prevalent method is GNNs, which learns node representations through recursive aggregation of information from neighboring nodes. However, based on the model of the message-passing mechanism, small noise propagation to neighboring areas may cause deterioration of the representation quality.

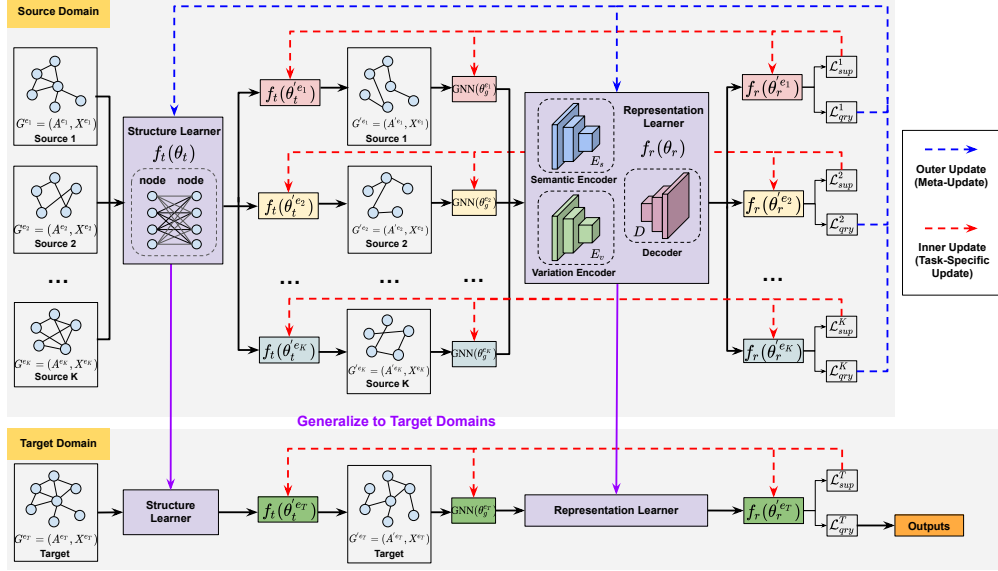


Figure 2: An overview of MLDGG. Each source graph is viewed as a task. For each task, the parameters  $\{\theta'_t, \theta'_g, \theta'_r\}$  of the structure learner ( $f_t$ ), GNN, and representation learner ( $f_r$ ) are updated via  $\mathcal{L}_{sup}$  during the inner update phase. Subsequently, the query losses  $\mathcal{L}_{qry}$  across all tasks are aggregated to update the meta-parameters  $\theta = \{\theta_t, \theta_r\}$  in the outer update phase. To generalize to graphs in the target domain, the learned meta-parameters of the structure learner and the representation learner are further fine-tuned for adaptation.

Therefore, we optimize GNN by learning high-quality graph structures. Further, we also explore the common structural pattern between cross-domain graphs to improve generalization ability. Here, we define a refined graph structure matrix as  $A'$  learned by a graph structure learner  $f_t$ . The  $f_t$  is expected to produce optimal graph structures that can give rise to satisfactory downstream classification performance.

First, we learn an intermediate similarity graph matrix  $F$ , where  $F_{jk}$  denotes the edge weights of node  $j$  and  $k$ . To fuse attributes and topological information, we use the representation of nodes  $\mathbf{r} \in \mathbb{R}^d$  to calculate the weight of edges between nodes:

$$F_{jk} = \delta(\mathbf{r}_j \odot \hat{\mathbf{w}}, \mathbf{r}_k \odot \hat{\mathbf{w}}), \quad (3)$$

where  $\hat{\mathbf{w}} \in \mathbb{R}^m$  is a weight vector and is trainable,  $\delta(\cdot, \cdot)$  is a similarity function that includes simple dot-product and so on. After obtaining  $F$ , we generate a novel graph structure  $A'$  by sampling from  $A'_{jk} \sim \text{Bernoulli}(F_{jk})$ . Further, we regularize the learned graph structure using sparsity and smoothness constraints:

$$\mathcal{B} = -\alpha \sum_{j,k} A'_{j,k} \|\mathbf{r}_j - \mathbf{r}_k\|_2^2 - \beta \|A'\|_0, \quad (4)$$

where the  $\alpha$  and  $\beta$  are hyperparameters controlling different modules' importance. We adopt the policy gradient optimization method for the non-differentiable problem of sampling  $A'$ . We define the probability for sampling as follows:

$$\Phi(A') = \prod_{j,k} (A'_{jk} F_{jk} + (1 - A'_{jk})(1 - F_{jk})). \quad (5)$$

Then we independently sample  $H$  times to obtain  $\{A'_h\}_{h=1}^H$  and  $\{\Phi(A'_h)\}_{h=1}^H$ . We define the regularization  $\mathcal{B}$  in Eq. (4) as the reward function, then we optimize the  $\theta_t$  using REINFORCE [58] algorithm with the gradient:

$$\nabla_{\theta_t} \mathcal{L}^{reg} = -\nabla_{\theta_t} \frac{1}{H} \sum_{h=1}^H \log \Phi(A'_h) (\mathcal{B}(A'_h) - \bar{\mathcal{B}}), \quad (6)$$

where  $\bar{\mathcal{B}}$  is the mean value, serving as a baseline function. It operates by averaging the regularization rewards  $\mathcal{B}(A')$  across a single feed-forward computation, thereby aiding in the reduction of variance throughout the training of the policy gradient.

After obtaining  $A'$  by structure learner  $f_t$ , we recursively propagate features along the latent graph  $A'$  and original adjacent matrix  $A$  to update node representations by the GNN network parameterized by  $\theta_g$ . This process can be formulated as:

$$R = \lambda \text{GNN}(R, A) + (1 - \lambda) \text{GNN}(R, A'), \quad (7)$$

where  $\lambda$  denotes the weight coefficient,  $R = \{\mathbf{r}_j\}_{j=1}^{|\mathcal{V}|} \in \mathbb{R}^{|\mathcal{V}| \times d}$  where  $\mathbf{r} \in \mathbb{R}^d$  is the node representation.

## 4.2 Representation Learner

Despite GNNs having the capability to extract abstract representations for predictions, the representation may unconsciously mix up semantic factors  $\mathbf{s}$  and variation factors  $\mathbf{v}$  due to a correlation between them. So the model still relies on the domain-specific variation factors  $\mathbf{v}$  for prediction via this correlation. However, this correlation may change drastically in a new domain, making the effect from  $\mathbf{v}$  misleading. So we assume the representation of each node is disentangled into two factors: a domain-invariant semantic factor  $\mathbf{s}$  determining the label and a domain-specific variation factor  $\mathbf{v}$  independent of labels.  $p(\mathbf{r}|\mathbf{s}, \mathbf{v})$  and  $p(\mathbf{y}|\mathbf{s})$  are invariant across domains, and the change of prior  $p(\mathbf{s}, \mathbf{v})$  is the only source of domain change. Based on the above causal generative principle, we develop the representation learner based on variational Bayes [59, 60]. Here, the representation of the node learned by GNN  $\mathbf{r}$  and the label  $\mathbf{y}$  are accessible variables and we have supervised data from the underlying representation  $p^*(\mathbf{r}, \mathbf{y})$  in the source domain. The log marginal likelihood of the  $\mathbf{r}$  and  $\mathbf{y}$  is as follows:

$$\log p(\mathbf{r}, \mathbf{y}) = \log \int \int p(\mathbf{s}, \mathbf{v}, \mathbf{r}, \mathbf{y}) ds d\mathbf{v}, \quad (8)$$

where  $p(\mathbf{s}, \mathbf{v}, \mathbf{r}, \mathbf{y}) := p(\mathbf{s}, \mathbf{v})p(\mathbf{r}|\mathbf{s}, \mathbf{v})p(\mathbf{y}|\mathbf{s})$ . By maximizing the likelihood in Eq. (8),  $p(\mathbf{r}, \mathbf{y})$  will match the  $p^*(\mathbf{r}, \mathbf{y})$ . However, the direct optimization of Eq. (8) is intractable, so we utilize the variational inference [60] to approximate the marginal likelihood. We introduce a tractable distribution  $q(\mathbf{s}, \mathbf{v}|\mathbf{r}, \mathbf{y})$  and construct the variational objective as follows:

$$\log p(\mathbf{r}, \mathbf{y}) \geq \mathbb{E}_{q(\mathbf{s}, \mathbf{v}|\mathbf{r}, \mathbf{y})} \left[ \log \frac{p(\mathbf{s}, \mathbf{v}, \mathbf{r}, \mathbf{y})}{q(\mathbf{s}, \mathbf{v}|\mathbf{r}, \mathbf{y})} \right] =: \mathcal{L}_{q_{\mathbf{s}, \mathbf{v}|\mathbf{r}, \mathbf{y}}}(\mathbf{r}, \mathbf{y}), \quad (9)$$

where  $\mathcal{L}_{p, q_{\mathbf{s}, \mathbf{v}|\mathbf{r}, \mathbf{y}}}(\mathbf{r}, \mathbf{y})$  is called Evidence Lower Bound (ELBO). Unfortunately, the introduced model  $q(\mathbf{s}, \mathbf{v}|\mathbf{r}, \mathbf{y})$  fails to facilitate the estimation of  $p(\mathbf{y}|\mathbf{r})$ . To alleviate this problem, we introduce an auxiliary model  $q(\mathbf{s}, \mathbf{v}, \mathbf{y}|\mathbf{r})$  to target  $p(\mathbf{s}, \mathbf{v}, \mathbf{y}|\mathbf{r})$ , which enables the straightforward sampling of  $\mathbf{y}$  given  $\mathbf{r}$  for prediction. Meanwhile,  $q(\mathbf{s}, \mathbf{v}, \mathbf{y}|\mathbf{r}) = q(\mathbf{s}, \mathbf{v}|\mathbf{r}, \mathbf{y})q(\mathbf{y}|\mathbf{r})$  means it can help learning inference model  $q(\mathbf{s}, \mathbf{v}|\mathbf{r}, \mathbf{y})$ , where  $q(\mathbf{y}|\mathbf{r}) := \int q(\mathbf{s}, \mathbf{v}, \mathbf{y}|\mathbf{r}) ds d\mathbf{v}$ . Due to  $p(\mathbf{s}, \mathbf{v}, \mathbf{y}|\mathbf{r})$  can be factorized as  $p(\mathbf{s}, \mathbf{v}|\mathbf{r})p(\mathbf{y}|\mathbf{s})$ . Thus, we can instead introduce a lighter inference  $q(\mathbf{s}, \mathbf{v}|\mathbf{r})$  for the minimally intractable component  $p(\mathbf{s}, \mathbf{v}|\mathbf{r})$  and use  $q(\mathbf{s}, \mathbf{v}|\mathbf{r})p(\mathbf{y}|\mathbf{s})$  as an approximation to  $q(\mathbf{s}, \mathbf{v}, \mathbf{y}|\mathbf{r})$ . This turns the objective Eq. (9) to:

$$\begin{aligned} \log p(\mathbf{r}, \mathbf{y}) &\geq \frac{1}{q(\mathbf{y}|\mathbf{r})} \left[ \mathbb{E}_{q(\mathbf{s}, \mathbf{v}|\mathbf{r})} [p(\mathbf{y}|\mathbf{s}) \log q(\mathbf{y}|\mathbf{r})] \right] \\ &\quad + \frac{1}{q(\mathbf{y}|\mathbf{r})} \left[ \mathbb{E}_{q(\mathbf{s}, \mathbf{v}|\mathbf{r})} [p(\mathbf{y}|\mathbf{s}) \log p(\mathbf{r}|\mathbf{s}, \mathbf{v})] \right] \\ &\quad + \frac{1}{q(\mathbf{y}|\mathbf{r})} \left[ \mathbb{E}_{q(\mathbf{s}, \mathbf{v}|\mathbf{r})} \left[ p(\mathbf{y}|\mathbf{s}) \log \frac{p(\mathbf{s}, \mathbf{v})}{q(\mathbf{s}, \mathbf{v}|\mathbf{r})} \right] \right] \\ &=: \mathcal{L}^{ELBO}, \end{aligned} \quad (10)$$

where  $q(\mathbf{y}|\mathbf{r}) = \mathbb{E}_{q(\mathbf{s}, \mathbf{v}|\mathbf{r})} [p(\mathbf{y}|\mathbf{s})]$ . The  $\mathcal{L}^{ELBO}$  in Eq. (10) consists of three components. The first term is the negative of the standard cross entropy (CE) loss and  $p(\mathbf{y}|\mathbf{s})$  gives the ability to model to predict the target label. The second term encourages the latent representation  $\mathbf{s}$  and  $\mathbf{v}$  to preserve the salient information of  $\mathbf{r}$  by reconstruction. The third and fourth term drives the variational posteriors  $q(\mathbf{s}, \mathbf{v}|\mathbf{r})$  towards its priors. By maximizing the  $\mathcal{L}^{ELBO}$  in Eq. (10), it becomes feasible to deduce the parameters of distribution over the joint latent variables  $\mathbf{s}$  and  $\mathbf{v}$ . The Monte Carlo method can be used to estimate expectations [59]. The derivation of Eq. (10) is provided in Appendix B.

**MLDGG-ind.** To improve the generalization of the model, we consider another case where  $\mathbf{s}$  and  $\mathbf{v}$  are independent, *i.e.*,  $p^\perp(\mathbf{s}, \mathbf{v}) = p(\mathbf{s})p(\mathbf{v})$ . Formally, the distribution  $p^\perp(\mathbf{s}, \mathbf{v})$  exhibits a higher entropy compared to  $p(\mathbf{s}, \mathbf{v})$ , which diminishes specific information of the source domain and promotes dependence on causal mechanisms for enhanced generalization. Under the conditional independence assumption, the  $p(\mathbf{s}, \mathbf{v})$  can be turned to  $p(\mathbf{s})p(\mathbf{v})$  and  $q(\mathbf{s}, \mathbf{v}|\mathbf{r})$  can be turned to  $q(\mathbf{s}|\mathbf{r})q(\mathbf{v}|\mathbf{r})$  in Eq. (10), which is denoted as  $\mathcal{L}_{ind}^{ELBO}$ .

### 4.2.1 Model in Detail.

We show the distributional assumption in MLDGG. For the prior  $p(\mathbf{s}, \mathbf{v})$ , we use a multivariate Gaussian distribution  $p(\mathbf{s}, \mathbf{v}) = \mathcal{N}((\mathbf{s}, \mathbf{v}) | (\mu_s, \mu_u), \Sigma)$ , where  $\mu_s$  and  $\mu_v$  are both zero vectors and  $\Sigma = \begin{pmatrix} \sum_{ss} & \sum_{sv} \\ \sum_{vs} & \sum_{vv} \end{pmatrix}$  is parameterized by its Cholesky decomposition [61]. For semantic encoder  $E_s$  and variation encoder  $E_v$ , we formulate their variational posterior distribution as Gaussian distribution with diagonal covariance structure, parameterized by neural network. For the decoder  $D$ , we adopt the Gaussian distribution  $q(\mathbf{s}, \mathbf{v} | \mathbf{r}) = \mathcal{N}(\mathbf{s}, \mathbf{v} | \mu_r, \sigma_r^2 I)$ , where  $\mu_r$  and  $\sigma_r$  are given by the mapping during reconstruct process. The semantic factor  $\mathbf{s} = E_s(\mathbf{r})$  is used to predict node label  $y$ , *i.e.*,  $\hat{y} = \hat{f}(\mathbf{s})$ , where  $\hat{f}$  is a classifier. The variation factor  $\mathbf{v} = E_v(\mathbf{r})$  is independent of label. MLDGG uses both  $\mathbf{s}$  and  $\mathbf{v}$  to reconstruct representation  $\mathbf{r}$ , *i.e.*,  $\mathbf{r} = D(\mathbf{s}, \mathbf{v})$ . For the prior  $p(\mathbf{s})$  and  $p(\mathbf{v})$  in MLDGG-ind, we adopt standard Gaussian  $\mathcal{N}(\mathbf{s}; 0, I)$  and  $\mathcal{N}(\mathbf{v}; 0, I)$ , respectively.

### 4.3 Meta-Learning

To learn a good parameter initialization of  $\theta = \{\theta_t, \theta_r\}$  across all given source graphs, we use the MAML [39] framework to integrate the structure learner with the representation learner. The objective function is:

$$\mathcal{L} = -\mathcal{L}^{ELBO} + \lambda_r \mathcal{L}^{reg}, \quad (11)$$

where  $\lambda_r$  is the weight coefficient of regularization loss. We randomly sampled the support set  $\mathcal{T}_{sup}^i$  and the query set  $\mathcal{T}_{qry}^i$  from the output of the semantic encoder  $E_s$  for each task  $i$ .

For the inner update, first, compute  $\mathcal{L}_{sup}^i$  on  $\mathcal{T}_{sup}^i$ , and then update its parameters  $\theta^{i}$  iteratively with  $\eta$  loops as follows:

$$\theta^{i} = \theta - l_{in} \nabla_{\theta} \mathcal{L}_{sup}^i, \quad (12)$$

where  $l_{in}$  is the inner learning rate and  $\theta^{i} = \{\theta_t^i, \theta_g^i, \theta_s^i, \theta_v^i, \theta_d^i\}$ .

For the outer update, we apply the parameters  $\theta^{i}$  that have been iteratively updated several times in the inner loop to its query set  $\mathcal{T}_{qry}^i$  to calculate the  $\mathcal{L}_{qry}^i$ . Then update  $\theta$  as follows:

$$\theta = \theta - l_{out} \nabla_{\theta} \frac{1}{M} \sum_{i=1}^M \mathcal{L}_{qry}^i, \quad (13)$$

where  $l_{out}$  is the learning rate of the outer loop and  $\theta = \{\theta_t, \theta_r\}$ . The process of our framework is in Algorithm 1. The complexity analysis of the algorithm is presented in Appendix B.1.

## 5 Theoretical Analysis

This section presents a theoretical analysis of the boundary guarantee for domain generalization errors in the meta-learning framework that integrates the structural and representation learner.

**Theorem 1** (Upper bound: accuracy). *Define the expected error of  $\hat{f}$  in representation space as  $\epsilon_{Acc}(\hat{f}) = \mathbb{E}[\mathcal{L}(\hat{f} \circ g(A, X), Y)]$ . For any  $\hat{f}: \mathbb{R}^s \rightarrow \mathbb{R}$ , any representation mapping  $g: \mathcal{A} \times \mathcal{X} \rightarrow \mathbb{R}^s$ , and any loss function  $\mathcal{L}: \mathbb{R} \times \mathbb{R} \rightarrow \mathbb{R}$  that is upper bounded by  $\pi_u$ , the expected error of  $\hat{f} \circ g: \mathcal{A} \times \mathcal{X} \rightarrow \mathbb{R}$  at any target domain  $e_T \in \mathcal{E}_t$  is upper bounded:*

$$\begin{aligned} \epsilon_{Acc}^{e_T}(\hat{f} \circ g) &\leq \frac{1}{K} \sum_{i=1}^K \epsilon_{Acc}^{e_i}(\hat{f} \circ g) + \sqrt{2 \mathbb{E}_{y \sim \mathbb{P}_Y^{e_i, j}} \left[ d_{JS}(\mathbb{P}_{S|Y}^{e_i}, \mathbb{P}_{S|Y}^{e_j})^2 \right]} \\ &+ \sqrt{2} \pi_u \max_{i \in [K]} d_{JS}(\mathbb{P}_{A, X, Y}^{e_T}, \mathbb{P}_{A, X, Y}^{e_i}) + \sqrt{2} \pi_u \max_{i, j \in [K]} d_{JS}(\mathbb{P}_Y^{e_i}, \mathbb{P}_Y^{e_j}). \end{aligned} \quad (14)$$

For simplicity, we omit parameters  $\theta$  and its domain  $\Theta$ . In this paper, the  $g$  function is  $g = f_t \circ \text{GNN} \circ E_s$ . We adopt Jensen-Shannon (JS) distance [62] denoted as  $d_{JS}$  to quantify the dissimilarity between two distributions.

**Theorem 2** (Lower bound: accuracy). *Suppose  $\mathcal{L}(\hat{f} \circ g(A, X), Y)$  is lower bounded by  $\pi_c$  when  $\hat{f} \circ g(A, X) \neq Y$ , and is 0 when  $\hat{f} \circ g(A, X) = Y$ . Let  $\xi$  denote the number of labels, if  $d_{JS}(\mathbb{P}_Y^{e_i}, \mathbb{P}_Y^{e_T}) \geq d_{JS}(\mathbb{P}_{A, X}^{e_i}, \mathbb{P}_{A, X}^{e_T})$ , the expected error of  $\hat{f}$  at source and target domains is lower bounded:*

$$\frac{1}{K} \sum_{i=1}^K \epsilon_{Acc}^{e_i}(\hat{f} \circ g) + \epsilon_{Acc}^{e_T}(\hat{f} \circ g) \geq \frac{\pi_c}{4\xi K} \sum_{i=1}^K \left( d_{JS}(\mathbb{P}_Y^{e_i}, \mathbb{P}_Y^{e_T}) - d_{JS}(\mathbb{P}_{A, X}^{e_i}, \mathbb{P}_{A, X}^{e_T}) \right)^4. \quad (15)$$

**Algorithm 1 The procedure of MLDGG**


---

```

1: Input: observed source graphs  $\{G^i\}_{i=1}^M$ , learning rates  $l_{in, out}$ 
2: Select  $M$  source graphs as tasks  $\{\mathcal{T}^i\}_{i=1}^M$ 
3: Initialize  $\theta_t, \theta_s, \theta_v, \theta_d$  and  $\{\theta_g^i\}_{i=1}^M$ 
4: While not done do:
5:   For each task  $\mathcal{T}^i$  do:
6:      $R_0^i = X^i$ 
7:     Compute  $F^i$  using Eq. (3)
8:     Sample  $H$  times over  $F^i$  to obtain  $A^i$ 
9:     Compute  $R^i$  using Eq. (7)
10:     $\theta_{t_0}^i = \theta_t, \theta_{s_0}^i = \theta_s, \theta_{v_0}^i = \theta_v, \theta_{d_0}^i = \theta_d, \theta_{g_0}^i = \theta_g^i$ 
11:    Sample  $\mathcal{T}_{qry}^i$  and  $\mathcal{T}_{sup}^i$ 
12:    For  $n$  in  $1, \dots, \eta$  do:
13:      Compute  $\mathcal{L}_{sup}^i$  on  $\mathcal{T}_{sup}^i$  via Eq. (11)
14:       $\theta_{t_n}^i = \theta_{t_{n-1}}^i - l_{in} \nabla \mathcal{L}_{sup}^i$ 
15:       $\theta_{s_n}^i = \theta_{s_{n-1}}^i - l_{in} \nabla \mathcal{L}_{sup}^i$ 
16:       $\theta_{v_n}^i = \theta_{v_{n-1}}^i - l_{in} \nabla \mathcal{L}_{sup}^i$ 
17:       $\theta_{d_n}^i = \theta_{d_{n-1}}^i - l_{in} \nabla \mathcal{L}_{sup}^i$ 
18:       $\theta_{g_n}^i = \theta_{g_{n-1}}^i - l_{in} \nabla \mathcal{L}_{sup}^i$ 
19:      Compute  $\mathcal{L}_{qry}^{i,n}$  on  $\mathcal{T}_{qry}^i$  via Eq. (11)
20:    End
21:     $\mathcal{L}_{qry}^i = \mathcal{L}_{qry}^{i,\eta}$ 
22:  End
23:  Update  $\theta_t \leftarrow \theta_t - l_{out} \nabla_{\theta_t} \frac{1}{M} \sum_{i=1}^M \mathcal{L}_{qry}^i$ 
24:  Update  $\theta_s \leftarrow \theta_s - l_{out} \nabla_{\theta_s} \frac{1}{M} \sum_{i=1}^M \mathcal{L}_{qry}^i$ 
25:  Update  $\theta_v \leftarrow \theta_v - l_{out} \nabla_{\theta_v} \frac{1}{M} \sum_{i=1}^M \mathcal{L}_{qry}^i$ 
26:  Update  $\theta_d \leftarrow \theta_d - l_{out} \nabla_{\theta_d} \frac{1}{M} \sum_{i=1}^M \mathcal{L}_{qry}^i$ 
27: End while
28: Output: trained initialization parameters  $\theta_t, \theta_s, \theta_v$  and  $\theta_d$ 

```

---

Theorem 2 indicates the infeasibility of optimizing the lower bound of error, which is determined by the dataset distribution, represented by  $A, X$ , and  $Y$ . The proof of Theorem 1 and Theorem 2 are provided in Appendix E.

To optimize the model on the target graph, we encounter the following issues: (C1) **Independent training of the GNNs**. A usual assumption is that the testing graph is the same as the training graph. This premise requires independently training the structure learning model from scratch for each graph dataset which leads to prohibitive computation costs and potential risks for serious over-fitting. (C2) **Distribution alignment**. Obtaining relatively domain-invariant semantic information in a disentangled manner is challenging when dealing with source domains with significant distribution differences. In other words, aligning  $\mathbb{P}_{S|Y}^{e_i}$  and  $\mathbb{P}_{S|Y}^{e_j}$  in the second part of Eq. (14) becomes difficult.

**Addressing (C1) by training the structure learner.** If we can learn from the  $A$  and  $X$  of source graphs how to capture structural information on the graph, we can then apply this ability to the target domain. Specifically, we decompose the representation mapping  $g : \mathcal{A}, \mathcal{X} \rightarrow \mathbb{R}^s$  in Theorem 1 into three parts:  $g = f_t \circ \text{GNN} \circ E_s$ , where  $f_t$  is a structure learner to refine the given structure (i.e.,  $A' = f_t(A, X)$ ), GNN embeds  $(A', X)$  and  $(A, X)$  to  $R$ , and  $E_s$  learns the semantic factor, i.e.,  $S = E_s(R)$ . Therefore, we can use this pre-trained  $f_t$  and  $E_s$  on the target graph instead of retraining the entire model. **Addressing (C2) by feature disentanglement.** To ensure the final classification, we aim to decouple domain-invariant information, which has a consistent distribution across each domain. In a perfect decoupling scenario, the second part of Eq. (14) would approach zero.

## 6 Experiments

We apply MLDGG to real-world datasets to investigate the effectiveness of domain generalization on graphs, which focuses on the following research questions.

- **RQ1:** Dose MLDGG surpass the the state-of-the-art methods in the field of domain generalization on graphs?



- **RQ2:** To what extent does each critical component contribute to the overall performance of the MLDGG?
- **RQ3:** How does the representation learner improve the generalization of GNN?

## 6.1 Experiment Setup

### 6.1.1 Datasets

We utilize three real network datasets that come with ground truth to verify the effectiveness of MLDGG. Experiments are conducted on the multiple graphs contained within each dataset. The statistical characteristics of these networks are shown in Table 1 and due to space constraints, we present the details of the dataset in the Appendix C.1.

Table 1: Key Characteristics of Datasets

Dataset	# Nodes	# Edges	# Classes	# Features	# Domains
TWITCH-EXPLICIT [25]	20945	153,138	2	3170	7 (DE, ENGB, ES, FR, PTBR, RU, and TW)
FACEBOOK-100 [26]	131,924	1,590,655	2	12412	5 (Amh, Johns, Reed, Cornel, and Yale)
WEBKB [27]	617	1138	5	1703	3 (Cornell, Texas, and Wis)

### 6.1.2 Baselines

We compare MLDGG with graph domain generation methods (EERM [16], SRGNN [63], FLOOD [15]), data augmentation methods for graphs (Mixup [64]), meta-learning methods for graphs (GMeta [44], GraphGlow[28], MD-Gram [57]) and a base method ERM. Readers can refer to Appendix C.2 for more details of baseline methods.

### 6.1.3 Implementation Details

We establish 3 different scenarios determined by whether the source and target graphs are derived from the same dataset.

- **S1T1.** Both source and target graphs originate from the same dataset. We sequentially test each graph for each dataset while training on the remaining ones.
- **S1T2.** The source graphs and target graphs are from different datasets. In particular, all graphs in the source are from the same dataset. For instance, we use 5 graphs from FACEBOOK-100 for training and testing on the graphs of TWITCH-EXPLICIT and WEBKB, separately. This approach can be similarly applied to other datasets.
- **S12T3.** The source graphs and target graphs are from different datasets. In particular, the source graphs for training are selected from different datasets. Here, we choose eight graphs from two distinct datasets for training (*e.g.*, FACEBOOK-100 and TWITCH-EXPLICIT), and testing on the other dataset (WEBKB).

We use GCN architectures as the GNN model in MLDGG. For all baseline models, we implemented them using the authors’ provided source code and also set GCN as the backbone. To reduce the time and space cost of the structure learner, following the simplification of [28], we convert the sampling of  $A'$  in the structure learner to the product of the (NP)-dimensional matrix and its transpose. Due to the baseline methods’ inability to adapt to varying feature and label dimensions, we employ zero-padding for feature dimensions and label expansion to standardize them after comparing different padding methods. We report the experimental results for all scenarios, with the final result for each dataset derived from the mean of all graphs within that dataset. The results represent the average values obtained from 10 runs for all the methods compared.

### 6.1.4 Hyper-parameter Settings

The parameters of the structure learner include  $\lambda$  (the weight on original graphs),  $\alpha$  (the weight on smoothness constraints), and  $\beta$  (the weight on sparsity constraints). We adjust all values to fall within the range of  $[0, 1]$ . In meta-training, we set the update step as 5. In meta-testing, we set the update step in  $\{1, 5, 10, 20, 30, 40\}$ . The learning rates for the inner and outer loops are set to  $l_{in} = 1e^{-3}$  and  $l_{out} = 1e^{-1}$ , respectively.

## 6.2 Results

**Performance Comparison.** In response to RQ1, we evaluate MLDGG’s performance on three scenarios in 6.1.3. The results are reported in Table 3-6, where numbers in bold represent the best results and underlined means second best. Based on these, we identified the following observations:

Table 2: Test accuracy (%) on TWITCH, FB-100 and WEBKB where source and target graphs from same dataset.

Methods	SITI (TWITCH → TWITCH)								SITI (FB-100 → FB-100)					
	PTBR	TW	RU	ES	FR	ENGB	DE	Avg	Amherst	Johns	Reed	Cornell	Yale	Avg
GraphGlow [28]	65.4 ± 0.6	60.7 ± 0.2	75.4 ± 0.5	70.7 ± 0.5	63.1 ± 0.2	54.5 ± 0.1	60.4 ± 0.9	64.3	53.0 ± 0.5	50.1 ± 0.9	61.2 ± 1.1	51.6 ± 0.3	50.9 ± 0.8	53.4
MD-Gram [57]	61.3 ± 1.2	59.2 ± 1.3	70.1 ± 0.9	65.7 ± 0.4	60.9 ± 0.6	53.3 ± 0.8	56.9 ± 1.0	61.1	51.9 ± 0.3	50.1 ± 0.8	59.9 ± 0.5	51.1 ± 0.4	49.0 ± 0.7	52.4
GMeta [44]	60.0 ± 0.1	59.4 ± 0.6	61.2 ± 0.4	63.5 ± 0.2	60.2 ± 0.4	49.8 ± 0.7	53.6 ± 0.1	58.2	46.4 ± 0.8	44.5 ± 1.0	48.9 ± 0.5	40.2 ± 0.1	46.8 ± 0.9	45.4
FLOOD [15]	57.0 ± 0.3	49.0 ± 0.4	46.1 ± 0.2	55.3 ± 0.4	50.4 ± 0.2	51.3 ± 0.3	53.1 ± 0.4	51.7	49.8 ± 0.3	47.1 ± 0.4	48.9 ± 0.6	41.0 ± 0.3	45.1 ± 0.2	46.4
EERM [16]	65.3 ± 0.0	60.7 ± 0.0	72.7 ± 3.8	70.9 ± 0.2	59.3 ± 4.4	46.6 ± 0.2	51.0 ± 1.1	60.9	53.9 ± 0.7	50.4 ± 1.7	51.8 ± 0.9	52.6 ± 1.1	52.9 ± 1.3	52.3
SRGNN [63]	38.8 ± 2.6	44.3 ± 3.7	58.8 ± 1.1	53.8 ± 1.5	48.4 ± 0.4	40.3 ± 2.0	44.9 ± 0.1	47.0	46.1 ± 1.3	47.9 ± 0.6	49.5 ± 1.0	46.1 ± 1.4	48.8 ± 0.9	47.7
Mixup [65]	45.1 ± 1.2	45.3 ± 0.9	39.9 ± 1.5	48.1 ± 1.3	42.6 ± 1.3	40.9 ± 0.6	46.2 ± 0.8	44.0	45.8 ± 0.6	46.1 ± 0.7	48.4 ± 0.2	47.2 ± 0.4	47.1 ± 0.2	46.9
ERM [66]	65.0 ± 0.2	58.6 ± 2.9	66.8 ± 3.5	70.1 ± 0.1	63.0 ± 0.1	45.2 ± 0.0	42.1 ± 0.9	58.7	44.6 ± 0.5	46.9 ± 0.9	47.8 ± 1.2	44.3 ± 1.0	50.1 ± 0.7	46.7
MLDGG	67.8 ± 0.3	61.5 ± 0.2	76.0 ± 0.1	71.4 ± 0.1	63.7 ± 0.2	55.0 ± 0.2	60.5 ± 0.1	65.1	55.2 ± 0.1	51.3 ± 0.1	62.9 ± 0.2	53.8 ± 0.2	54.0 ± 0.2	55.5
MLDGG-ind	<b>67.9 ± 0.8</b>	<b>62.0 ± 0.1</b>	<b>76.1 ± 0.1</b>	<b>71.5 ± 0.3</b>	<b>64.8 ± 0.2</b>	<b>55.5 ± 0.3</b>	<b>61.9 ± 0.5</b>	<b>65.7</b>	<b>55.5 ± 0.1</b>	<b>51.4 ± 0.3</b>	<b>64.2 ± 0.1</b>	<b>54.2 ± 0.4</b>	<b>54.3 ± 0.5</b>	<b>55.9</b>

Methods	SITI (WEBKB → WEBKB)			
	Texas	Cornell	Wis	Avg
GraphGlow [28]	57.3 ± 2.1	44.8 ± 1.5	46.3 ± 0.6	49.5
MD-Gram [57]	55.8 ± 0.6	43.9 ± 0.7	45.2 ± 0.7	48.3
GMeta [44]	42.3 ± 0.7	20.5 ± 1.9	40.1 ± 0.4	34.3
FLOOD [15]	22.5 ± 0.6	18.7 ± 0.2	15.6 ± 0.1	18.9
EERM [16]	31.1 ± 2.1	19.2 ± 1.3	7.7 ± 1.7	19.3
SRGNN [63]	14.3 ± 2.8	15.8 ± 0.6	18.7 ± 2.5	16.3
Mixup [65]	14.0 ± 1.2	16.2 ± 1.0	17.9 ± 1.6	16.0
ERM [66]	42.8 ± 3.9	12.8 ± 2.0	13.5 ± 1.2	23.0
MLDGG	56.6 ± 0.2	47.3 ± 0.3	51.7 ± 0.3	51.9
MLDGG-ind	<b>59.7 ± 0.3</b>	<b>49.6 ± 0.2</b>	<b>54.0 ± 0.2</b>	<b>54.4</b>

First, MLDGG exhibits superior performance compared with other competitive baselines on all datasets within three experimental settings, highlighting its robust generalization capabilities. The structure learner guides the model to learn more meaningful node representations and capture shared structure information across domains, and the representation learner guides the model to disentangle semantic and domain-specific information in node representation. Furthermore, we have observed superior classification performance when  $s$  and  $v$  are independent. This observation suggests that domain-specific and label-independent variation factors disturb the model’s classification, consequently influencing its generalization capability. Disentangling  $s$  and  $v$  offers greater advantages for generalization.

Second, the results of S1T1, S1T2, and S1T3 demonstrate that the best generalization performance is achieved when the training domain originates from diverse datasets. Among all comparative methods, the performance of GraphGlow is second only to our framework, which suggests that integrating structure learning with GNN facilitates the capture of richer knowledge within graphs. All comparative methods exhibit varying performances under different distribution shift settings. Traditional invariant learning methods exhibit superior performance in scenarios where the source domain originates from the same dataset, as opposed to situations involving diverse datasets. It suggests that invariant learning methods demonstrate limited generalization ability in situations with substantial distribution shifts. Other cross-domain meta-learning methods do show better generalization ability for cross-domain scenarios. In contrast, cross-domain meta-learning methods demonstrate superior performance, attributable to meta-learning’s advanced ability to capture shared knowledge across domains.

**Ablation Studies.** To answer RQ2, we conduct five ablation studies to evaluate the robustness of key modules, namely structure learner, representation learner, and MAML. The results of MLDGG and MLDGG-ind are shown in Fig. 3 and Fig. 4, where we follow the setting of Table 6. In-depth descriptions and the algorithms for these studies and more results can be found in Appendix D. (1) In MLDGG w/o SL, we input the graph directly into the GNN to learn node representations and compare its accuracy with MLDGG. We observe declines of 2% to 3% in accuracy across all settings compared to the full model. Given that GNNs often aggregate task-irrelevant information, which can result in overfitting and diminish generalization performance, the introduction of the structure learner becomes crucial. By mitigating the adverse effects of task-unrelated edges, the structure learner facilitates the acquisition of comprehensive node representations, thereby improving the overall performance. (2) In MLDGG w/o RL, we only keep the structure learner and just finetune the GNN encoder during the test phase. We observe a more substantial loss in performance degradation to 3% to 6% across all settings. This indicates that the disentanglement of semantic and variation factors can enhance the model’s generalization capability. Class labels are dependent on semantic factors, while variation factors representing domain-specific elements are not associated with these labels. When the representation learner is absent, performance degradation occurs, particularly in the presence of OOD samples stemming from distributional shifts in target domains. Therefore, mitigating the influence of variation factors becomes crucial for improving the model’s robustness across diverse domains. (3) In MLDGG w/o MAML, it does not share the semantic and variation encoders across different domains, which significantly decreases model performance by 8% to 10%. This observation indicates the critical role played by the meta-learner modules in facilitating knowledge transfer from source and target graphs. The MAML framework serves as an integration for both the structure learner and representation learner,

Table 3: Test accuracy (%) on FB-100 and WEBKB where all source graphs from TWITCH.

Methods	SIT2 ( Twitch $\rightarrow$ FB-100 )						SIT2 ( Twitch $\rightarrow$ WebKB )			
	Amherst	Johns	Reed	Cornell	Yale	Avg	Texas	Cornell	Wis	Avg
GraphGlow [28]	52.9 $\pm$ 1.5	52.3 $\pm$ 1.2	60.7 $\pm$ 1.7	51.2 $\pm$ 1.0	43.5 $\pm$ 1.2	52.1	53.0 $\pm$ 1.1	44.8 $\pm$ 1.3	47.0 $\pm$ 0.9	48.3
MD-Gram [57]	50.2 $\pm$ 0.3	47.9 $\pm$ 0.4	62.8 $\pm$ 0.4	49.0 $\pm$ 0.2	42.7 $\pm$ 0.7	50.5	53.8 $\pm$ 0.2	41.6 $\pm$ 0.3	44.2 $\pm$ 0.3	46.5
GMeta [44]	20.1 $\pm$ 0.8	14.5 $\pm$ 1.7	16.0 $\pm$ 1.6	16.9 $\pm$ 1.4	16.3 $\pm$ 2.1	16.8	19.8 $\pm$ 1.7	16.0 $\pm$ 1.4	16.2 $\pm$ 1.3	17.3
FLOOD [15]	11.1 $\pm$ 0.3	14.0 $\pm$ 0.4	11.9 $\pm$ 0.3	14.2 $\pm$ 0.2	14.3 $\pm$ 0.5	13.1	19.3 $\pm$ 0.2	17.2 $\pm$ 0.4	11.0 $\pm$ 0.3	15.8
EERM [16]	10.9 $\pm$ 2.4	14.3 $\pm$ 3.1	12.8 $\pm$ 2.0	13.0 $\pm$ 2.6	14.4 $\pm$ 3.0	13.1	20.8 $\pm$ 2.3	18.0 $\pm$ 2.5	11.2 $\pm$ 1.9	16.7
SRGNN [63]	11.7 $\pm$ 1.3	15.0 $\pm$ 1.8	11.6 $\pm$ 1.5	12.7 $\pm$ 1.4	13.9 $\pm$ 2.6	13.0	16.7 $\pm$ 1.9	11.4 $\pm$ 0.6	10.8 $\pm$ 1.5	13.0
Mixup [65]	10.8 $\pm$ 1.7	12.9 $\pm$ 1.0	12.1 $\pm$ 1.3	11.3 $\pm$ 1.2	13.2 $\pm$ 1.5	12.1	17.5 $\pm$ 1.1	10.9 $\pm$ 1.4	11.1 $\pm$ 1.3	13.2
ERM [66]	18.9 $\pm$ 2.0	10.2 $\pm$ 1.6	11.6 $\pm$ 2.2	19.0 $\pm$ 2.1	11.9 $\pm$ 1.8	12.3	20.2 $\pm$ 1.4	15.5 $\pm$ 2.5	10.6 $\pm$ 4.4	15.4
MLDGG	55.5 $\pm$ 0.4	51.4 $\pm$ 0.5	64.1 $\pm$ 0.2	52.4 $\pm$ 0.2	53.5 $\pm$ 0.3	55.4	58.1 $\pm$ 0.1	50.4 $\pm$ 0.2	51.1 $\pm$ 0.2	53.2
MLDGG-ind	<b>55.3 <math>\pm</math> 0.5</b>	<b>51.9 <math>\pm</math> 1.2</b>	<b>64.0 <math>\pm</math> 1.1</b>	<b>53.5 <math>\pm</math> 0.7</b>	<b>54.0 <math>\pm</math> 0.8</b>	<b>55.7</b>	<b>59.5 <math>\pm</math> 0.2</b>	<b>48.9 <math>\pm</math> 0.1</b>	<b>51.5 <math>\pm</math> 0.1</b>	<b>53.3</b>

Table 4: Test accuracy (%) on TWITCH and WEBKB where source graphs all from FB-100.

Methods	SIT2 ( FB-100 $\rightarrow$ Twitch )							SIT2 ( FB-100 $\rightarrow$ WebKB )				
	PTBR	TW	RU	ES	FR	ENGB	DE	Avg	Texas	Cornell	Wis	Avg
GraphGlow [28]	65.4 $\pm$ 0.4	60.7 $\pm$ 0.6	75.4 $\pm$ 0.9	70.7 $\pm$ 0.9	63.1 $\pm$ 0.7	54.5 $\pm$ 0.6	60.4 $\pm$ 0.8	64.3	59.0 $\pm$ 0.5	44.8 $\pm$ 0.4	46.6 $\pm$ 0.9	50.1
MD-Gram [57]	64.8 $\pm$ 0.3	58.7 $\pm$ 0.4	73.0 $\pm$ 0.1	71.1 $\pm$ 0.9	62.0 $\pm$ 0.4	52.9 $\pm$ 0.5	60.1 $\pm$ 0.5	63.2	54.1 $\pm$ 0.4	44.8 $\pm$ 0.7	45.0 $\pm$ 0.2	48.0
GMeta [44]	10.5 $\pm$ 1.9	26.6 $\pm$ 1.4	14.8 $\pm$ 2.2	7.1 $\pm$ 1.4	23.7 $\pm$ 2.4	13.3 $\pm$ 1.0	15.8 $\pm$ 2.5	15.9	20.0 $\pm$ 1.9	15.8 $\pm$ 2.0	18.6 $\pm$ 1.7	18.1
FLOOD [15]	11.4 $\pm$ 0.3	24.3 $\pm$ 0.2	18.1 $\pm$ 0.2	10.2 $\pm$ 0.6	24.8 $\pm$ 0.1	11.9 $\pm$ 0.4	16.0 $\pm$ 0.4	19.1	18.3 $\pm$ 0.1	16.9 $\pm$ 0.3	11.0 $\pm$ 0.4	15.4
EERM [16]	11.4 $\pm$ 2.4	29.8 $\pm$ 2.5	17.0 $\pm$ 1.8	6.3 $\pm$ 2.7	25.0 $\pm$ 2.9	12.3 $\pm$ 2.4	16.9 $\pm$ 2.9	17.0	17.5 $\pm$ 2.8	12.6 $\pm$ 2.9	10.8 $\pm$ 1.3	13.6
SRGNN [63]	18.3 $\pm$ 1.6	15.9 $\pm$ 2.0	15.0 $\pm$ 1.8	18.1 $\pm$ 1.2	14.7 $\pm$ 2.0	10.5 $\pm$ 1.8	11.4 $\pm$ 1.4	15.0	18.0 $\pm$ 1.1	10.7 $\pm$ 1.4	11.5 $\pm$ 1.2	13.4
Mixup [65]	19.7 $\pm$ 1.0	27.5 $\pm$ 1.9	16.4 $\pm$ 1.2	17.0 $\pm$ 1.8	19.6 $\pm$ 1.6	12.0 $\pm$ 2.1	13.8 $\pm$ 1.7	18.1	19.7 $\pm$ 1.5	12.6 $\pm$ 1.0	12.8 $\pm$ 0.9	15.0
ERM [66]	16.7 $\pm$ 1.3	27.0 $\pm$ 2.9	15.0 $\pm$ 3.4	13.5 $\pm$ 2.6	14.3 $\pm$ 2.2	15.7 $\pm$ 3.1	14.3 $\pm$ 2.0	15.9	33.5 $\pm$ 3.7	38.2 $\pm$ 3.0	30.1 $\pm$ 1.5	33.9
MLDGG	66.7 $\pm$ 0.1	61.2 $\pm$ 0.2	76.5 $\pm$ 0.2	71.9 $\pm$ 0.2	64.0 $\pm$ 0.3	55.0 $\pm$ 0.1	60.8 $\pm$ 0.3	65.2	56.6 $\pm$ 0.2	48.1 $\pm$ 0.3	48.9 $\pm$ 0.2	51.2
MLDGG-ind	<b>67.1 <math>\pm</math> 0.2</b>	<b>61.8 <math>\pm</math> 0.1</b>	<b>76.5 <math>\pm</math> 0.1</b>	<b>71.9 <math>\pm</math> 0.3</b>	<b>64.0 <math>\pm</math> 0.2</b>	<b>55.6 <math>\pm</math> 0.1</b>	<b>61.1 <math>\pm</math> 0.2</b>	<b>65.4</b>	<b>60.5 <math>\pm</math> 0.4</b>	<b>48.3 <math>\pm</math> 0.2</b>	<b>52.3 <math>\pm</math> 0.2</b>	<b>53.7</b>

thereby enabling efficient knowledge transfer and facilitating effective adaptation to unseen target domains. (4) In MLDGG w/o INNER-SL, we remove each task-specific structure learner so that all tasks share a structure learner. We observe declines of 1% to 2% in accuracy across all settings compared to the full model. This indicates that learning initialization parameters for the structure learner based on the meta-learning framework are conducive to capturing the structure information shared by different domains and improving the generalization ability. (5) In MLDGG w/o INNER-RL, we remove each task-specific representation learner so that all tasks share a representation learner, which decreases model performance by 2% to 3%. This indicates that learning initialization parameters for the representation learner based on the meta-learning framework can guide the model to learn semantic factors and variation factors, to better disentangle to improve generalization ability.

**The demonstration of the effectiveness of the representation learner.** To answer RQ3, we visualize the output  $\mathbf{r}$  of each node of the GNN, domain-invariant semantic factors  $\mathbf{s}$  and domain-specific variation factors  $\mathbf{v}$  respectively in Fig. 5 (different colors represent different labels). The domain-invariant semantic factors  $\mathbf{s}$  and domain-specific variation factors  $\mathbf{v}$  are disentangled from the node representations  $\mathbf{r}$  learned from GNNs. We can see that the samples represented by  $\mathbf{s}$  are more distinguished than those represented by  $\mathbf{r}$ . The samples represented by  $\mathbf{v}$  are independent of classes. These phenomena indicate that by disentangling the node representation learned from GNN to capture the domain-invariant semantic information that determines the label, the influence of the variation factors on the label prediction can be reduced and better generalization performance can be achieved.

**Sensitivity Analysis.** The results of sensitivity analysis of MLDGG to varying numbers of gradient steps during meta-testing and the weight of the original graph  $\lambda$  are provided in Appendix F.1.

## 7 Conclusion

In this paper, we introduce a novel cross-multi-domain meta-learning framework, MLDGG, for node-level graph domain generalization. The framework integrates a structure and a representation learner within the meta-learning paradigm to facilitate knowledge transfer and enable rapid adaptation to target domains previously. The structure learner mitigates the adverse effects of task-unrelated edges to facilitate the acquisition of comprehensive node representations of GNN while capturing the shared structure information. The representation learner by disentangling the semantic and variation factors enhances the model’s generalization. We conduct extensive experiments and the results demonstrate that our model outperforms baseline methods.

Table 5: Test accuracy (%) on TWITCH and FB-100 where source graphs all from WEBKB.

Methods	S1T2 (WebKB $\rightarrow$ Twitch)									S1T2 (WebKB $\rightarrow$ FB-100)					
	PTBR	TW	RU	ES	FR	ENGB	DE	Avg	Amherst	Johns	Reed	Cornell	Yale	Avg	
GraphGlow [28]	65.4 $\pm$ 1.1	60.7 $\pm$ 1.3	75.4 $\pm$ 0.9	70.7 $\pm$ 0.3	63.1 $\pm$ 1.2	54.5 $\pm$ 0.2	60.4 $\pm$ 0.5	64.3	52.7 $\pm$ 1.8	51.3 $\pm$ 1.0	61.7 $\pm$ 1.2	51.3 $\pm$ 1.5	52.4 $\pm$ 1.3	53.8	
MD-Gram [57]	64.3 $\pm$ 0.4	57.8 $\pm$ 0.3	72.0 $\pm$ 0.4	70.7 $\pm$ 0.8	61.4 $\pm$ 0.5	52.2 $\pm$ 0.6	58.9 $\pm$ 0.5	62.5	51.1 $\pm$ 0.4	48.0 $\pm$ 0.3	62.9 $\pm$ 0.6	48.7 $\pm$ 0.3	44.2 $\pm$ 0.6	51.0	
GMeta [44]	12.7 $\pm$ 2.1	23.5 $\pm$ 1.3	28.9 $\pm$ 1.4	30.8 $\pm$ 1.7	13.0 $\pm$ 2.1	15.2 $\pm$ 1.8	19.3 $\pm$ 1.2	22.3	29.7 $\pm$ 1.5	26.6 $\pm$ 2.0	19.8 $\pm$ 0.9	21.5 $\pm$ 1.8	20.4 $\pm$ 1.2	23.6	
FLOOD [15]	10.0 $\pm$ 0.3	28.5 $\pm$ 0.4	28.1 $\pm$ 0.3	31.4 $\pm$ 0.2	20.9 $\pm$ 0.1	11.8 $\pm$ 0.2	16.7 $\pm$ 0.5	21.0	40.7 $\pm$ 1.0	39.9 $\pm$ 0.4	39.0 $\pm$ 0.3	45.5 $\pm$ 0.4	41.2 $\pm$ 0.8	41.3	
EERM [16]	10.1 $\pm$ 3.3	31.1 $\pm$ 2.5	30.8 $\pm$ 2.7	34.1 $\pm$ 2.9	22.8 $\pm$ 3.5	13.9 $\pm$ 2.1	15.4 $\pm$ 0.8	22.6	42.8 $\pm$ 2.7	41.4 $\pm$ 2.6	40.6 $\pm$ 2.8	49.1 $\pm$ 3.5	43.8 $\pm$ 2.6	43.5	
SRGNN [63]	11.2 $\pm$ 0.9	29.6 $\pm$ 1.4	28.5 $\pm$ 1.7	31.9 $\pm$ 2.0	24.1 $\pm$ 2.2	13.4 $\pm$ 1.3	16.1 $\pm$ 1.0	22.1	21.2 $\pm$ 1.8	19.6 $\pm$ 1.7	18.3 $\pm$ 0.9	20.9 $\pm$ 1.7	21.6 $\pm$ 1.5	20.3	
Mixup [65]	12.0 $\pm$ 1.3	27.5 $\pm$ 1.7	27.9 $\pm$ 1.6	31.4 $\pm$ 1.5	25.0 $\pm$ 1.9	14.2 $\pm$ 1.6	16.3 $\pm$ 1.0	22.0	32.6 $\pm$ 2.0	31.7 $\pm$ 1.2	29.9 $\pm$ 0.8	32.0 $\pm$ 1.9	30.1 $\pm$ 1.6	31.3	
ERM [66]	34.5 $\pm$ 2.9	10.5 $\pm$ 0.4	41.1 $\pm$ 4.8	20.7 $\pm$ 3.3	16.8 $\pm$ 0.2	12.6 $\pm$ 0.2	15.0 $\pm$ 0.1	21.7	40.9 $\pm$ 2.6	46.0 $\pm$ 2.1	40.5 $\pm$ 2.4	42.1 $\pm$ 2.6	44.4 $\pm$ 3.8	42.7	
MLDGG	66.2 $\pm$ 0.3	61.8 $\pm$ 0.1	75.9 $\pm$ 0.2	71.3 $\pm$ 0.2	63.9 $\pm$ 0.1	55.1 $\pm$ 0.3	60.3 $\pm$ 0.3	64.9	55.7 $\pm$ 0.1	51.5 $\pm$ 0.2	65.0 $\pm$ 0.1	53.1 $\pm$ 0.4	53.5 $\pm$ 0.2	55.8	
MLDGG-ind	66.8 $\pm$ 0.5	61.8 $\pm$ 0.2	76.5 $\pm$ 0.2	71.8 $\pm$ 0.1	63.9 $\pm$ 0.1	55.2 $\pm$ 0.4	61.1 $\pm$ 0.2	65.3	55.7 $\pm$ 0.3	51.7 $\pm$ 0.6	65.0 $\pm$ 0.4	53.9 $\pm$ 0.6	53.6 $\pm$ 0.5	56.0	

Table 6: Test accuracy (%) on TWITCH, FB-100 and WEBKB where source and target graphs from different datasets.

Methods	S1T3 (FB-100 + WebKB $\rightarrow$ Twitch)									S1T3 (Twitch + WebKB $\rightarrow$ FB-100)					
	PTBR	TW	RU	ES	FR	ENGB	DE	Avg	Amherst41	Johns	Reed	Cornell	Yale	Avg	
GraphGlow [28]	65.4 $\pm$ 0.5	60.7 $\pm$ 0.4	75.4 $\pm$ 0.4	70.7 $\pm$ 0.4	63.1 $\pm$ 0.3	54.5 $\pm$ 1.0	60.4 $\pm$ 0.7	64.3	53.1 $\pm$ 0.8	47.4 $\pm$ 1.2	63.2 $\pm$ 1.1	50.9 $\pm$ 1.1	43.4 $\pm$ 1.1	51.6	
MD-Gram [57]	65.1 $\pm$ 0.3	60.9 $\pm$ 0.1	73.9 $\pm$ 0.2	71.0 $\pm$ 0.2	62.6 $\pm$ 0.2	53.8 $\pm$ 0.1	60.2 $\pm$ 0.4	63.9	50.8 $\pm$ 0.7	48.3 $\pm$ 0.4	63.3 $\pm$ 0.5	49.9 $\pm$ 0.4	43.1 $\pm$ 0.7	51.1	
GMeta [44]	31.9 $\pm$ 1.8	24.0 $\pm$ 1.2	27.6 $\pm$ 1.8	31.0 $\pm$ 2.1	22.8 $\pm$ 1.6	26.0 $\pm$ 1.1	20.2 $\pm$ 1.9	26.2	21.3 $\pm$ 2.1	23.2 $\pm$ 1.7	19.9 $\pm$ 1.6	22.2 $\pm$ 1.7	21.5 $\pm$ 1.4	21.6	
FLOOD [15]	24.9 $\pm$ 0.6	11.7 $\pm$ 0.4	24.1 $\pm$ 0.7	15.0 $\pm$ 0.3	13.9 $\pm$ 0.4	13.0 $\pm$ 0.3	14.1 $\pm$ 0.4	16.7	19.1 $\pm$ 0.1	16.5 $\pm$ 0.3	12.0 $\pm$ 0.3	25.6 $\pm$ 0.4	15.8 $\pm$ 0.2	17.8	
EERM [16]	26.5 $\pm$ 2.1	12.3 $\pm$ 3.1	25.8 $\pm$ 2.8	15.4 $\pm$ 2.9	14.8 $\pm$ 2.8	13.5 $\pm$ 3.0	14.6 $\pm$ 2.7	17.6	19.9 $\pm$ 4.1	17.1 $\pm$ 2.9	12.1 $\pm$ 4.3	26.6 $\pm$ 3.1	16.9 $\pm$ 2.2	18.5	
SRGNN [63]	11.3 $\pm$ 1.2	28.4 $\pm$ 1.0	27.7 $\pm$ 2.1	29.6 $\pm$ 1.2	25.3 $\pm$ 1.6	12.7 $\pm$ 1.9	17.3 $\pm$ 1.5	21.7	18.2 $\pm$ 1.8	18.0 $\pm$ 1.6	10.6 $\pm$ 2.3	24.9 $\pm$ 1.8	15.5 $\pm$ 1.3	17.4	
Mixup [65]	12.3 $\pm$ 1.7	25.5 $\pm$ 1.4	26.9 $\pm$ 2.0	30.4 $\pm$ 1.2	24.0 $\pm$ 0.7	13.1 $\pm$ 0.5	17.5 $\pm$ 1.3	21.4	16.3 $\pm$ 1.6	13.6 $\pm$ 1.9	13.2 $\pm$ 2.2	22.5 $\pm$ 1.4	14.2 $\pm$ 1.8	16.0	
ERM [66]	26.1 $\pm$ 2.9	15.0 $\pm$ 2.6	6.4 $\pm$ 2.1	13.8 $\pm$ 0.4	17.4 $\pm$ 2.8	15.2 $\pm$ 3.6	14.0 $\pm$ 2.6	15.6	19.3 $\pm$ 0.1	24.5 $\pm$ 3.9	10.5 $\pm$ 2.7	25.0 $\pm$ 2.1	12.7 $\pm$ 2.8	18.4	
MLDGG	66.6 $\pm$ 0.4	61.4 $\pm$ 0.3	75.8 $\pm$ 0.3	71.3 $\pm$ 0.2	63.2 $\pm$ 0.3	55.1 $\pm$ 0.5	62.3 $\pm$ 0.5	65.1	55.5 $\pm$ 0.3	51.5 $\pm$ 0.5	64.5 $\pm$ 0.5	53.2 $\pm$ 0.1	53.6 $\pm$ 0.2	55.7	
MLDGG-ind	68.3 $\pm$ 0.6	62.9 $\pm$ 0.4	77.1 $\pm$ 0.5	72.6 $\pm$ 0.5	65.0 $\pm$ 0.2	56.1 $\pm$ 0.6	63.0 $\pm$ 0.5	66.4	55.7 $\pm$ 0.5	52.0 $\pm$ 0.6	64.6 $\pm$ 0.8	54.0 $\pm$ 0.2	54.2 $\pm$ 0.3	56.1	

Methods	S1T3 (FB-100 + Twitch $\rightarrow$ WebKB)			
	Texas	Cornell	Wis	Avg
GraphGlow [28]	55.2 $\pm$ 0.9	44.8 $\pm$ 1.2	45.4 $\pm$ 1.0	48.5
MD-Gram [57]	55.4 $\pm$ 0.5	45.2 $\pm$ 0.3	45.1 $\pm$ 0.6	48.6
GMeta [44]	23.2 $\pm$ 1.4	21.9 $\pm$ 1.9	19.6 $\pm$ 2.0	21.6
FLOOD [15]	19.7 $\pm$ 0.3	18.1 $\pm$ 0.4	15.5 $\pm$ 0.4	17.8
EERM [16]	20.7 $\pm$ 0.0	18.3 $\pm$ 0.4	13.9 $\pm$ 0.0	17.6
SRGNN [63]	19.2 $\pm$ 1.8	15.7 $\pm$ 1.6	14.0 $\pm$ 1.3	16.3
Mixup [65]	18.1 $\pm$ 1.6	13.9 $\pm$ 2.1	13.2 $\pm$ 1.2	15.1
ERM [66]	21.3 $\pm$ 0.9	16.4 $\pm$ 2.8	15.2 $\pm$ 2.0	17.3
MLDGG	58.2 $\pm$ 0.1	50.4 $\pm$ 0.3	52.3 $\pm$ 0.3	53.6
MLDGG-ind	62.0 $\pm$ 0.2	50.6 $\pm$ 0.5	51.2 $\pm$ 0.4	54.6

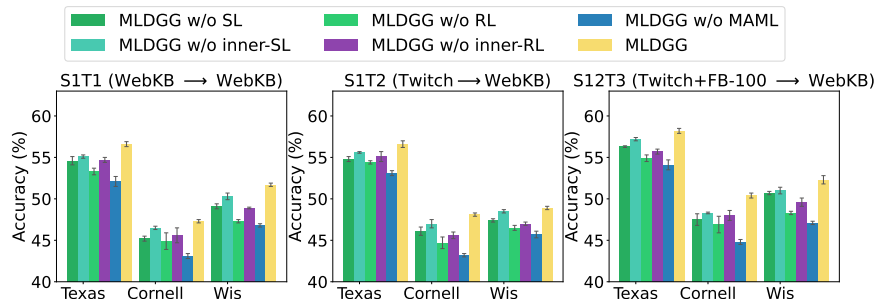


Figure 3: Ablation study for MLDGG under three distinct cross-domain scenarios.

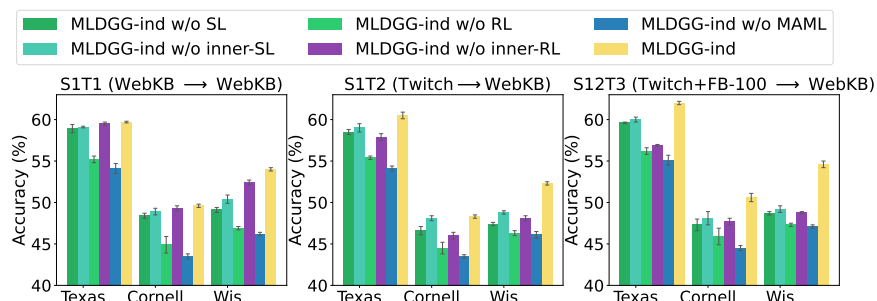


Figure 4: Ablation study for MLDGG-ind under three distinct cross-domain scenarios.

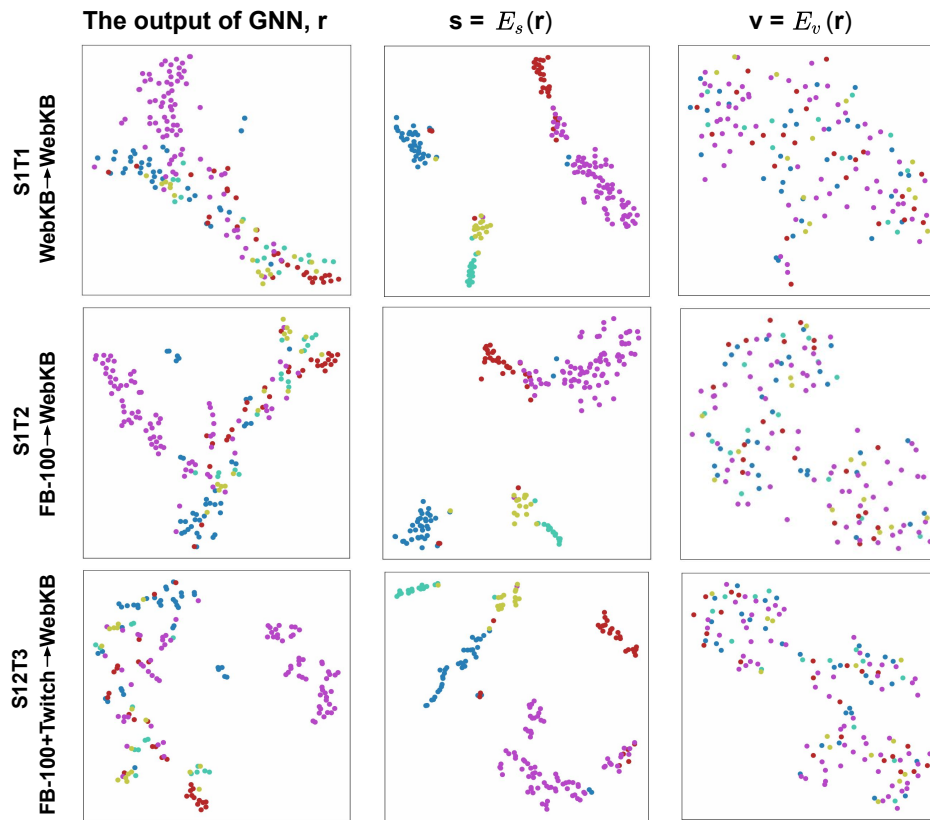


Figure 5: The demonstration of the effectiveness of representation learner on 3 different setting **S12T3**, **S1T2**, and **S1T1** using T-sne visualization.  $\mathbf{r}$  denotes the output of GNN,  $\mathbf{s} = E_s(\mathbf{r})$  denotes the semantic factor and  $\mathbf{v} = E_v(\mathbf{r})$  denotes the variation factor. Different colors represent different labels.

## References

- [1] Krikamol Muandet, David Balduzzi, and Bernhard Schölkopf. Domain generalization via invariant feature representation. In *International conference on machine learning*, pages 10–18. PMLR, 2013.
- [2] Haoliang Li, Sinno Jialin Pan, Shiqi Wang, and Alex C Kot. Domain generalization with adversarial feature learning. In *Proceedings of the IEEE conference on computer vision and pattern recognition*, pages 5400–5409, 2018.
- [3] Minglai Shao, Dong Li, Chen Zhao, Xintao Wu, Yujie Lin, and Qin Tian. Supervised algorithmic fairness in distribution shifts: A survey. *arXiv preprint arXiv:2402.01327*, 2024.
- [4] Chen Zhao, Kai Jiang, Xintao Wu, Haoliang Wang, Latifur Khan, Christan Grant, and Feng Chen. Algorithmic fairness generalization under covariate and dependence shifts simultaneously. In *Proceedings of the 30th ACM SIGKDD Conference on Knowledge Discovery and Data Mining*, pages 4419–4430, 2024.
- [5] Chen Zhao, Feng Mi, Xintao Wu, Kai Jiang, Latifur Khan, and Feng Chen. Dynamic environment responsive online meta-learning with fairness awareness. *ACM Transactions on Knowledge Discovery from Data*, 18(6):1–23, 2024.
- [6] Dong Li, Chen Zhao, Minglai Shao, and Wenjun Wang. Learning fair invariant representations under covariate and correlation shifts simultaneously. In *Proceedings of the 33rd ACM International Conference on Information and Knowledge Management*, pages 1174–1183, 2024.
- [7] Yujie Lin, Chen Zhao, Minglai Shao, Baoluo Meng, Xujiang Zhao, and Haifeng Chen. Towards counterfactual fairness-aware domain generalization in changing environments. *IJCAI*, 2024.
- [8] Yujie Lin, Chen Zhao, Minglai Shao, Xujiang Zhao, and Haifeng Chen. Adaptation speed analysis for fairness-aware causal models. In *Proceedings of the 32nd ACM International Conference on Information and Knowledge Management*, pages 1421–1430, 2023.
- [9] Chen Zhao, Feng Mi, Xintao Wu, Kai Jiang, Latifur Khan, Christan Grant, and Feng Chen. Towards fair disentangled online learning for changing environments. In *Proceedings of the ACM SIGKDD Conference on Knowledge Discovery and Data Mining*, 2023.
- [10] Chen Zhao, Feng Mi, Xintao Wu, Kai Jiang, Latifur Khan, and Feng Chen. Adaptive fairness-aware online meta-learning for changing environments. In *Proceedings of the 28th ACM SIGKDD Conference on Knowledge Discovery and Data Mining*, pages 2565–2575, 2022.
- [11] Chen Zhao, Feng Chen, and Bhavani Thuraisingham. Fairness-aware online meta-learning. In *Proceedings of the 27th ACM SIGKDD Conference on Knowledge Discovery & Data Mining*, pages 2294–2304, 2021.
- [12] Kai Jiang, Chen Zhao, Haoliang Wang, and Feng Chen. Feed: Fairness-enhanced meta-learning for domain generalization. *arXiv preprint arXiv:2411.01316*, 2024.
- [13] Divyat Mahajan, Shruti Tople, and Amit Sharma. Domain generalization using causal matching. In *International conference on machine learning*, pages 7313–7324. PMLR, 2021.
- [14] Fangrui Lv, Jian Liang, Shuang Li, Bin Zang, Chi Harold Liu, Ziteng Wang, and Di Liu. Causality inspired representation learning for domain generalization. In *Proceedings of the IEEE/CVF conference on computer vision and pattern recognition*, pages 8046–8056, 2022.
- [15] Yang Liu, Xiang Ao, Fuli Feng, Yunshan Ma, Kuan Li, Tat-Seng Chua, and Qing He. Flood: A flexible invariant learning framework for out-of-distribution generalization on graphs. In *Proceedings of the 29th ACM SIGKDD Conference on Knowledge Discovery and Data Mining*, pages 1548–1558, 2023.
- [16] Qitian Wu, Hengrui Zhang, Junchi Yan, and David Wipf. Handling distribution shifts on graphs: An invariance perspective. *arXiv preprint arXiv:2202.02466*, 2022.
- [17] Hyeonjin Park, Seunghun Lee, Sihyeon Kim, Jinyoung Park, Jisu Jeong, Kyung-Min Kim, Jung-Woo Ha, and Hyunwoo J Kim. Metropolis-hastings data augmentation for graph neural networks. *Advances in Neural Information Processing Systems*, 34:19010–19020, 2021.
- [18] Kezhi Kong, Guohao Li, Mucong Ding, Zuxuan Wu, Chen Zhu, Bernard Ghanem, Gavin Taylor, and Tom Goldstein. Robust optimization as data augmentation for large-scale graphs. In *Proceedings of the IEEE/CVF Conference on Computer Vision and Pattern Recognition*, pages 60–69, 2022.
- [19] Yongduo Sui, Xiang Wang, Jiancan Wu, An Zhang, and Xiangnan He. Adversarial causal augmentation for graph covariate shift. *arXiv preprint arXiv:2211.02843*, 2022.

- [20] Yingjun Du, Jun Xu, Huan Xiong, Qiang Qiu, Xiantong Zhen, Cees GM Snoek, and Ling Shao. Learning to learn with variational information bottleneck for domain generalization. In *Computer Vision–ECCV 2020: 16th European Conference, Glasgow, UK, August 23–28, 2020, Proceedings, Part X 16*, pages 200–216. Springer, 2020.
- [21] Mengyue Yang, Furui Liu, Zhitang Chen, Xinwei Shen, Jianye Hao, and Jun Wang. Causalvae: Disentangled representation learning via neural structural causal models. In *Proceedings of the IEEE/CVF conference on computer vision and pattern recognition*, pages 9593–9602, 2021.
- [22] Yongduo Sui, Xiang Wang, Jiancan Wu, Min Lin, Xiangnan He, and Tat-Seng Chua. Causal attention for interpretable and generalizable graph classification. In *Proceedings of the 28th ACM SIGKDD Conference on Knowledge Discovery and Data Mining*, pages 1696–1705, 2022.
- [23] Haoyang Li, Ziwei Zhang, Xin Wang, and Wenwu Zhu. Learning invariant graph representations for out-of-distribution generalization. *Advances in Neural Information Processing Systems*, 35:11828–11841, 2022.
- [24] Qitian Wu, Yiting Chen, Chenxiao Yang, and Junchi Yan. Energy-based out-of-distribution detection for graph neural networks. In *International Conference on Learning Representations (ICLR)*, 2023.
- [25] Benedek Rozemberczki, Carl Allen, and Rik Sarkar. Multi-scale attributed node embedding. *Journal of Complex Networks*, 9(2):cnab014, 2021.
- [26] Amanda L Traud, Peter J Mucha, and Mason A Porter. Social structure of facebook networks. *Physica A: Statistical Mechanics and its Applications*, 391(16):4165–4180, 2012.
- [27] Hongbin Pei, Bingzhe Wei, Kevin Chen-Chuan Chang, Yu Lei, and Bo Yang. Geom-gcn: Geometric graph convolutional networks. *arXiv preprint arXiv:2002.05287*, 2020.
- [28] Wentao Zhao, Qitian Wu, Chenxiao Yang, and Junchi Yan. Graphglow: Universal and generalizable structure learning for graph neural networks. *arXiv preprint arXiv:2306.11264*, 2023.
- [29] Alexander Robey, George J Pappas, and Hamed Hassani. Model-based domain generalization. *Advances in Neural Information Processing Systems*, 34:20210–20229, 2021.
- [30] Vikas Garg, Adam Tauman Kalai, Katrina Ligett, and Steven Wu. Learn to expect the unexpected: Probably approximately correct domain generalization. In *International Conference on Artificial Intelligence and Statistics*, pages 3574–3582. PMLR, 2021.
- [31] Kaiyang Zhou, Ziwei Liu, Yu Qiao, Tao Xiang, and Chen Change Loy. Domain generalization: A survey. *IEEE Transactions on Pattern Analysis and Machine Intelligence*, 2022.
- [32] Qi Qian, Shenghuo Zhu, Jiasheng Tang, Rong Jin, Baigui Sun, and Hao Li. Robust optimization over multiple domains. In *Proceedings of the AAAI Conference on Artificial Intelligence*, volume 33, pages 4739–4746, 2019.
- [33] Shiori Sagawa, Pang Wei Koh, Tatsunori B Hashimoto, and Percy Liang. Distributionally robust neural networks for group shifts: On the importance of regularization for worst-case generalization. *arXiv preprint arXiv:1911.08731*, 2019.
- [34] David Krueger, Ethan Caballero, Joern-Henrik Jacobsen, Amy Zhang, Jonathan Binas, Dinghuai Zhang, Remi Le Priol, and Aaron Courville. Out-of-distribution generalization via risk extrapolation (rex). In *International Conference on Machine Learning*, pages 5815–5826. PMLR, 2021.
- [35] Da Li, Yongxin Yang, Yi-Zhe Song, and Timothy Hospedales. Learning to generalize: Meta-learning for domain generalization. In *Proceedings of the AAAI conference on artificial intelligence*, volume 32, 2018.
- [36] Keyu Chen, Di Zhuang, and J Morris Chang. Discriminative adversarial domain generalization with meta-learning based cross-domain validation. *Neurocomputing*, 467:418–426, 2022.
- [37] Kaveh Hassani. Cross-domain few-shot graph classification. In *Proceedings of the AAAI Conference on Artificial Intelligence*, volume 36, pages 6856–6864, 2022.
- [38] Yiming Zhang, Yiyue Qian, Yanfang Ye, and Chuxu Zhang. Adapting distilled knowledge for few-shot relation reasoning over knowledge graphs. In *Proceedings of the 2022 SIAM International Conference on Data Mining (SDM)*, pages 666–674. SIAM, 2022.
- [39] Chelsea Finn, Pieter Abbeel, and Sergey Levine. Model-agnostic meta-learning for fast adaptation of deep networks. In *International conference on machine learning*, pages 1126–1135. PMLR, 2017.
- [40] Ricardo Vilalta and Youssef Drissi. A perspective view and survey of meta-learning. *Artificial intelligence review*, 18:77–95, 2002.

- [41] Da Li, Jianshu Zhang, Yongxin Yang, Cong Liu, Yi-Zhe Song, and Timothy M Hospedales. Episodic training for domain generalization. In *Proceedings of the IEEE/CVF International Conference on Computer Vision*, pages 1446–1455, 2019.
- [42] Yogesh Balaji, Swami Sankaranarayanan, and Rama Chellappa. Metareg: Towards domain generalization using meta-regularization. *Advances in neural information processing systems*, 31, 2018.
- [43] Qi Dou, Daniel Coelho de Castro, Konstantinos Kamnitsas, and Ben Glocker. Domain generalization via model-agnostic learning of semantic features. *Advances in neural information processing systems*, 32, 2019.
- [44] Kexin Huang and Marinka Zitnik. Graph meta learning via local subgraphs. *Advances in neural information processing systems*, 33:5862–5874, 2020.
- [45] Fan Zhou, Chengtai Cao, Kunpeng Zhang, Goce Trajcevski, Ting Zhong, and Ji Geng. Meta-gnn: On few-shot node classification in graph meta-learning. In *Proceedings of the 28th ACM International Conference on Information and Knowledge Management*, pages 2357–2360, 2019.
- [46] Huaxiu Yao, Chuxu Zhang, Ying Wei, Meng Jiang, Suhang Wang, Junzhou Huang, Nitesh Chawla, and Zhenhui Li. Graph few-shot learning via knowledge transfer. In *Proceedings of the AAAI conference on artificial intelligence*, volume 34, pages 6656–6663, 2020.
- [47] Ning Wang, Minnan Luo, Kaize Ding, Lingling Zhang, Jundong Li, and Qinghua Zheng. Graph few-shot learning with attribute matching. In *Proceedings of the 29th ACM International Conference on Information & Knowledge Management*, pages 1545–1554, 2020.
- [48] Ning Ma, Jiajun Bu, Jieyu Yang, Zhen Zhang, Chengwei Yao, Zhi Yu, Sheng Zhou, and Xifeng Yan. Adaptive-step graph meta-learner for few-shot graph classification. In *Proceedings of the 29th ACM International Conference on Information & Knowledge Management*, pages 1055–1064, 2020.
- [49] Zhichun Guo, Chuxu Zhang, Wenhao Yu, John Herr, Olaf Wiest, Meng Jiang, and Nitesh V Chawla. Few-shot graph learning for molecular property prediction. In *Proceedings of the web conference 2021*, pages 2559–2567, 2021.
- [50] Flood Sung, Yongxin Yang, Li Zhang, Tao Xiang, Philip HS Torr, and Timothy M Hospedales. Learning to compare: Relation network for few-shot learning. In *Proceedings of the IEEE conference on computer vision and pattern recognition*, pages 1199–1208, 2018.
- [51] Zhen Tan, Kaize Ding, Ruocheng Guo, and Huan Liu. Graph few-shot class-incremental learning. In *Proceedings of the Fifteenth ACM International Conference on Web Search and Data Mining*, pages 987–996, 2022.
- [52] Chelsea Finn, Kelvin Xu, and Sergey Levine. Probabilistic model-agnostic meta-learning. *Advances in neural information processing systems*, 31, 2018.
- [53] Yaqing Wang, Quanming Yao, James T Kwok, and Lionel M Ni. Generalizing from a few examples: A survey on few-shot learning. *ACM computing surveys (csur)*, 53(3):1–34, 2020.
- [54] Jürgen Schmidhuber. *Evolutionary principles in self-referential learning, or on learning how to learn: the meta-meta-... hook*. PhD thesis, Technische Universität München, 1987.
- [55] Fengchun Qiao, Long Zhao, and Xi Peng. Learning to learn single domain generalization. In *Proceedings of the IEEE/CVF conference on computer vision and pattern recognition*, pages 12556–12565, 2020.
- [56] Antreas Antoniou, Harri Edwards, and Amos Storkey. How to train your maml. In *Seventh International Conference on Learning Representations*, 2019.
- [57] Mingkai Lin, Wenzhong Li, Ding Li, Yizhou Chen, Guohao Li, and Sanglu Lu. Multi-domain generalized graph meta learning. In *Proceedings of the AAAI Conference on Artificial Intelligence*, volume 37, pages 4479–4487, 2023.
- [58] Junzi Zhang, Jongho Kim, Brendan O’Donoghue, and Stephen Boyd. Sample efficient reinforcement learning with reinforce. In *Proceedings of the AAAI conference on artificial intelligence*, volume 35, pages 10887–10895, 2021.
- [59] Diederik P Kingma and Max Welling. Auto-encoding variational bayes. *arXiv preprint arXiv:1312.6114*, 2013.
- [60] Michael I Jordan, Zoubin Ghahramani, Tommi S Jaakkola, and Lawrence K Saul. An introduction to variational methods for graphical models. *Machine learning*, 37:183–233, 1999.
- [61] Nicholas J Higham. Analysis of the cholesky decomposition of a semi-definite matrix. 1990.
- [62] Dominik Maria Endres and Johannes E Schindelin. A new metric for probability distributions. *IEEE Transactions on Information theory*, 49(7):1858–1860, 2003.



- [63] Qi Zhu, Natalia Ponomareva, Jiawei Han, and Bryan Perozzi. Shift-robust gnns: Overcoming the limitations of localized graph training data. *Advances in Neural Information Processing Systems*, 34:27965–27977, 2021.
- [64] Yiwei Wang, Wei Wang, Yuxuan Liang, Yujun Cai, and Bryan Hooi. Mixup for node and graph classification. In *Proceedings of the Web Conference 2021*, pages 3663–3674, 2021.
- [65] Hongyi Zhang, Moustapha Cisse, Yann N Dauphin, and David Lopez-Paz. mixup: Beyond empirical risk minimization. *arXiv preprint arXiv:1710.09412*, 2017.
- [66] Thomas N Kipf and Max Welling. Semi-supervised classification with graph convolutional networks. *arXiv preprint arXiv:1609.02907*, 2016.

## A Notations

For clear interpretation, we list the notations used in this paper and their corresponding explanation, as shown in Table 7.

Table 7: Important notations and corresponding descriptions.

Notations	Descriptions
$\mathcal{G}$	A set of graphs
$e_i$	The $i$ -th source domain
$e_T$	The target domain
$G^{e_i}$	A graph from domain $e_i$
$A^{e_i}$	The adjacency matrix of $G^{e_i}$
$X^{e_i}$	The node feature matrix of $G^{e_i}$
$\mathbf{y}^{e_i}$	The label of $G^{e_i}$
$\mathcal{V}^{e_i}$	A collection of nodes in $G^{e_i}$
$F$	The similarity matrix of nodes
$R$	The representation matrix of nodes in a graph $G$
$A'$	The learned adjacency matrix of structure learner
$\mathcal{E}$	The set of domains
$\mathcal{E}_s$	The set of source domains
$\mathcal{E}_t$	The set of target domains
$D$	The dimension of node feature
$\mathcal{T}$	The set of tasks in meta-learning
$\mathbf{s}$	The semantic factors
$\mathbf{v}$	The variation factors
$\mathbf{r}$	The output of GNN
$E_s$	The semantic encoder
$E_v$	The variation encoder
$\hat{f} \circ g$	A classifier
$f_t$	The structure learner
$f_r$	The Representation learner
$\theta_t$	The initialization parameters of a structure learner
$\theta_r$	The initialization parameters of a representation learner
$\theta_s$	The parameters of a semantic encoder
$\theta_v$	The parameters of a variation encoder
$\theta_d$	The parameters of a decoder
$\theta_g$	The parameters of GNNs
$\lambda$	The weight of the original graph
$\lambda_r$	The weight coefficient of regularization loss
$l_{in}, l_{out}$	The inner loop and outer loop learning rate, respectively
$M$	The number of tasks
$K$	The number of source graphs

## B Model Details

**The Evidence Lower Bound (ELBO).** In this paper, we assume the representation of each node is disentangled into two factors: a domain-invariant semantic factor  $\mathbf{s}$  determining the label and a domain-specific variation factor  $\mathbf{v}$  independent of labels. A common and effective approach for aligning the model  $p$  with the data distribution  $p^*(\mathbf{r}, \mathbf{y})$  is through maximizing likelihood  $p(\mathbf{r}, \mathbf{y}) = \log p(\mathbf{r}, \mathbf{y})$ . With these two latent variables, the log marginal likelihood can be  $\log \int \int p(\mathbf{s}, \mathbf{v}, \mathbf{r}, \mathbf{y}) dsdv$ . However, this is an intractable problem that is difficult to evaluate and optimize. To address this problem, one plausible way is to introduce a variational distribution  $q(\mathbf{s}, \mathbf{v}|\mathbf{r}, \mathbf{y})$ , conditioned on the observed variables based on variational expectation-maximization (variational EM). Then, a lower bound of the likelihood function can be derived:

$$\begin{aligned} \log p(\mathbf{r}, \mathbf{y}) &= \log \mathbb{E}_{q(\mathbf{s}, \mathbf{v}|\mathbf{r}, \mathbf{y})} \left[ \frac{p(\mathbf{s}, \mathbf{v}, \mathbf{r}, \mathbf{y})}{q(\mathbf{s}, \mathbf{v}|\mathbf{r}, \mathbf{y})} \right] \\ &\geq \mathbb{E}_{q(\mathbf{s}, \mathbf{v}|\mathbf{r}, \mathbf{y})} \left[ \log \frac{p(\mathbf{s}, \mathbf{v}, \mathbf{r}, \mathbf{y})}{q(\mathbf{s}, \mathbf{v}|\mathbf{r}, \mathbf{y})} \right] \\ &=: \mathcal{L}_{q_{\mathbf{s}, \mathbf{v}|\mathbf{r}, \mathbf{y}}}(\mathbf{r}, \mathbf{y}) \end{aligned} \quad (16)$$

where  $\mathcal{L}_{q_{\mathbf{s}, \mathbf{v}|\mathbf{r}, \mathbf{y}}}(\mathbf{r}, \mathbf{y})$  is called Evidence Lower Bound (ELBO). The variational distribution  $q(\mathbf{s}, \mathbf{v}|\mathbf{r}, \mathbf{y})$  is commonly instantiated by a standalone model and is regarded as an inference model. Unfortunately, the introduced model  $q(\mathbf{s}, \mathbf{v}|\mathbf{r}, \mathbf{y})$  fails to facilitate the estimation of  $p(\mathbf{y}|\mathbf{r})$ . To alleviate this problem, we introduce an auxiliary model  $q(\mathbf{s}, \mathbf{v}, \mathbf{y}|\mathbf{r})$  to target  $p(\mathbf{s}, \mathbf{v}, \mathbf{y}|\mathbf{r})$ , which enables the straightforward sampling of  $\mathbf{y}$  given  $\mathbf{r}$  for prediction. Meanwhile,  $q(\mathbf{s}, \mathbf{v}|\mathbf{r}, \mathbf{y}) = \frac{q(\mathbf{s}, \mathbf{v}, \mathbf{y}|\mathbf{r})}{q(\mathbf{y}|\mathbf{r})}$  means  $q(\mathbf{s}, \mathbf{v}, \mathbf{y}|\mathbf{r})$  can help learning inference model  $q(\mathbf{s}, \mathbf{v}|\mathbf{r}, \mathbf{y})$ , where  $q(\mathbf{y}|\mathbf{r}) := \int q(\mathbf{s}, \mathbf{v}, \mathbf{y}|\mathbf{r}) dsdv$ . When the ELBO approaches its maximum, all posterior items gradually tend to converge towards the prior, thus  $q(\mathbf{s}, \mathbf{v}, \mathbf{y}|\mathbf{r}) = p(\mathbf{s}, \mathbf{v}, \mathbf{y}|\mathbf{r}) = p(\mathbf{s}, \mathbf{v}|\mathbf{r})p(\mathbf{y}|\mathbf{s})$ . For  $p(\mathbf{s}, \mathbf{v}|\mathbf{r})$ , we instead use inference model  $q(\mathbf{s}, \mathbf{v}|\mathbf{r})$ . Then,  $q(\mathbf{s}, \mathbf{v}|\mathbf{r}, \mathbf{y}) = \frac{q(\mathbf{s}, \mathbf{v}|\mathbf{r})p(\mathbf{y}|\mathbf{s})}{q(\mathbf{y}|\mathbf{r})}$ . Then, the ELBO is turned to:

$$\begin{aligned} &\mathbb{E}_{q(\mathbf{s}, \mathbf{v}|\mathbf{r}, \mathbf{y})} \left[ \log \frac{p(\mathbf{s}, \mathbf{v}, \mathbf{r}, \mathbf{y})}{q(\mathbf{s}, \mathbf{v}|\mathbf{r}, \mathbf{y})} \right] \\ &= \mathbb{E}_{q(\mathbf{s}, \mathbf{v}|\mathbf{r}, \mathbf{y})} \left[ \log \frac{p(\mathbf{s}, \mathbf{v}, \mathbf{r}, \mathbf{y})q(\mathbf{y}|\mathbf{r})}{q(\mathbf{s}, \mathbf{v}|\mathbf{r})p(\mathbf{y}|\mathbf{s})} \right] \\ &= \mathbb{E}_{q(\mathbf{s}, \mathbf{v}|\mathbf{r}, \mathbf{y})} \left[ \log \frac{p(\mathbf{s}, \mathbf{v})p(\mathbf{r}|\mathbf{s}, \mathbf{v})p(\mathbf{y}|\mathbf{s})q(\mathbf{y}|\mathbf{r})}{q(\mathbf{s}, \mathbf{v}|\mathbf{r})p(\mathbf{y}|\mathbf{s})} \right] \\ &= \mathbb{E}_{\frac{q(\mathbf{s}, \mathbf{v}|\mathbf{r})p(\mathbf{y}|\mathbf{s})}{q(\mathbf{y}|\mathbf{r})}} \left[ \log \frac{p(\mathbf{s}, \mathbf{v})p(\mathbf{r}|\mathbf{s}, \mathbf{v})p(\mathbf{y}|\mathbf{s})q(\mathbf{y}|\mathbf{r})}{q(\mathbf{s}, \mathbf{v}|\mathbf{r})p(\mathbf{y}|\mathbf{s})} \right] \\ &= \mathbb{E}_{\frac{q(\mathbf{s}, \mathbf{v}|\mathbf{r})p(\mathbf{y}|\mathbf{s})}{q(\mathbf{y}|\mathbf{r})}} \left[ \log \frac{p(\mathbf{s}, \mathbf{v})p(\mathbf{r}|\mathbf{s}, \mathbf{v})}{q(\mathbf{s}, \mathbf{v}|\mathbf{r})} + \log q(\mathbf{y}|\mathbf{r}) \right] \\ &= \mathbb{E}_{q(\mathbf{s}, \mathbf{v}|\mathbf{r})p(\mathbf{y}|\mathbf{s})} \left[ \frac{1}{q(\mathbf{y}|\mathbf{r})} \log q(\mathbf{y}|\mathbf{r}) \right] + \mathbb{E}_{q(\mathbf{s}, \mathbf{v}|\mathbf{r})p(\mathbf{y}|\mathbf{s})} \left[ \frac{1}{q(\mathbf{y}|\mathbf{r})} \log \frac{p(\mathbf{s}, \mathbf{v})p(\mathbf{r}|\mathbf{s}, \mathbf{v})}{q(\mathbf{s}, \mathbf{v}|\mathbf{r})} \right] \\ &= \mathbb{E}_{q(\mathbf{s}, \mathbf{v}|\mathbf{r})} \left[ \frac{p(\mathbf{y}|\mathbf{s}) \log q(\mathbf{y}|\mathbf{r})}{q(\mathbf{y}|\mathbf{r})} \right] + \mathbb{E}_{q(\mathbf{s}, \mathbf{v}|\mathbf{r})} \left[ \frac{p(\mathbf{y}|\mathbf{s})}{q(\mathbf{y}|\mathbf{r})} \left( \log p(\mathbf{r}|\mathbf{s}, \mathbf{v}) + \log \frac{p(\mathbf{s}, \mathbf{v})}{q(\mathbf{s}, \mathbf{v}|\mathbf{r})} \right) \right] \\ &= \frac{1}{q(\mathbf{y}|\mathbf{r})} \left[ \mathbb{E}_{q(\mathbf{s}, \mathbf{v}|\mathbf{r})} [p(\mathbf{y}|\mathbf{s}) \log q(\mathbf{y}|\mathbf{r})] + \mathbb{E}_{q(\mathbf{s}, \mathbf{v}|\mathbf{r})} [p(\mathbf{y}|\mathbf{s}) \log p(\mathbf{r}|\mathbf{s}, \mathbf{v})] \right] \\ &\quad + \frac{1}{q(\mathbf{y}|\mathbf{r})} \left[ \mathbb{E}_{q(\mathbf{s}, \mathbf{v}|\mathbf{r})} \left[ p(\mathbf{y}|\mathbf{s}) \log \frac{p(\mathbf{s}, \mathbf{v})}{q(\mathbf{s}, \mathbf{v}|\mathbf{r})} \right] \right] \end{aligned} \quad (17)$$

where  $q(\mathbf{y}|\mathbf{r}) = \mathbb{E}_{q(\mathbf{s}, \mathbf{v}|\mathbf{r})} [p(\mathbf{y}|\mathbf{s})]$ .

### B.1 Complexity Analysis

In our experiments followed by [28], the complexity of the structure learner is  $O(NP)$ , where  $P$  is the number of pivot nodes. The complexity of GCNs is  $O(|E|Dd)$ , where  $|E|$  and  $d$  are the number of edges and classes,  $D$  is the dimension of the node feature, respectively. The complexity of the representation learner is  $O(N)$ . Therefore, the complexity of our model is  $O(K(NP + \eta(|E|Dd + N)))$ , where  $K$  is the number of source domains and  $K, P, \eta \ll N$ , and  $D, d \ll |E|$ .

## C Datasets And Experimental Details

### C.1 Datasets

- **TWITCH-EXPLICIT** [25]. It is a gamer network that includes seven networks: DE, ENGB, ES, FR, PTBR, RU, and TW. Each network represents a particular game region. The aforementioned networks have comparable sizes but vary in terms of densities and maximum node degrees.
- **FACEBOOK-100** [26]. This dataset comprises 100 snapshots of the *Facebook* friendship network, dating back to 2005. Each node represents a user from a particular American university, and the edges indicate the friendships between these users. We use five networks in our experiments: Amherst, John Hopkins, Reed98, Cornell5, and Yale4.
- **WEBKB** [27]. It is a web page network dataset. The nodes in the network represent web pages, and the edges symbolize hyperlinks connecting these web pages. Additionally, the node features are represented using the bag-of-words representation of the web pages. The task is to classify the nodes into one of five categories: student, project, course, staff, and faculty. According to the university, it is split into three networks: Cornell, Texas, and Wisconsin.

### C.2 Baseline

- **EERM** [16] generates environments with diverse topologies and then minimizes the variances and mean values of predicted loss across different environments.
- **SRGNN** [63] is devoted to solving the distributional shift problem by converting biased data sets to unbiased data distribution.
- **Mixup** [65] improves model generation capacity by constructing novel training examples drawn from raw data, thereby expanding the training distribution.
- **GraphGlow** [28] employs a meta-learning approach to cultivate a generalized structure learner aimed at discerning universally applicable patterns in optimal messaging topologies across diverse datasets.
- **GMeta** [44] exhibits the capacity to generalize to Graph Neural Networks (GNNs) applied to entirely new graphs and labels that have not been encountered previously. Simultaneously, it showcases the ability to find evidence supporting predictions based on small datasets within local subgraphs surrounding target nodes or edges.
- **FLOOD** [15] employs an adaptive encoder, refined through invariant learning and bootstrapped learning strategies, to enhance performance on a test set. First, it constructs a shared encoder by minimizing the empirical risk across various domains. Then, it utilizes bootstrapped learning with a self-supervised method to tailor the shared encoder for optimal adaptation to the test set.
- **MD-Gram** [57] is a multi-domain graph meta-learning approach, transforming learning tasks from multiple source-domain graphs into a unified domain. This process facilitates the acquisition of transferable knowledge across domains.

## D Ablation Studies

We conduct five ablation studies, and detailed algorithms of designed ablation studies are given in Algorithms 2 to 6.

## E Theoretical Gurantee

**JS distance.** We adopt Jensen-Shannon (JS) distance [62] to measure the dissimilarity between two distributions. Formally, JS distance between distributions  $\mathbb{P}$  and  $\mathbb{P}'$  is defined as

$$d_{JS}(\mathbb{P}, \mathbb{P}') := \sqrt{\mathcal{D}_{JS}(\mathbb{P} || \mathbb{P}')} ,$$

where  $\mathcal{D}_{JS}(\mathbb{P} || \mathbb{P}') := \frac{1}{2} \mathcal{D}_{KL}(\mathbb{P} || \frac{\mathbb{P} + \mathbb{P}'}{2}) + \frac{1}{2} \mathcal{D}_{KL}(\mathbb{P}' || \frac{\mathbb{P} + \mathbb{P}'}{2})$  is JS divergence defined based on Kullback–Leibler (KL) divergence  $\mathcal{D}_{KL}(\cdot || \cdot)$ . Note that, unlike KL divergence, JS divergence is symmetric and bounded:  $0 \leq \mathcal{D}_{JS}(\mathbb{P} || \mathbb{P}') \leq 1$ .

### E.1 Proof for Theorem 1

*Proof.* Taking the average of upper bounds based on all source domains, we can have:

**Algorithm 2 MLDGG W/O SL (Ablation Study 1)**


---

```

1: While not done do:
2:   For each source graph  $\mathcal{T}^i$  do:
3:      $R_0^i = X^i$ 
4:      $\theta_{s_0}^i = \theta_s, \theta_{v_0}^i = \theta_v, \theta_{d_0}^i = \theta_d, \theta_{g_0}^i = \theta_g$ 
5:     Sample  $\mathcal{T}_{qry}^i$  and  $\mathcal{T}_{sup}^i$ 
6:     For  $n$  in  $1, \dots, \eta$  do:
7:       Compute  $\mathcal{L}_{sup}^i$  on  $\mathcal{T}_{sup}^i$  via Eq. (11)
8:        $\theta_{s_n}^i = \theta_{s_{n-1}}^i - l_{in} \nabla \mathcal{L}_{sup}^i$ 
9:        $\theta_{v_n}^i = \theta_{v_{n-1}}^i - l_{in} \nabla \mathcal{L}_{sup}^i$ 
10:       $\theta_{d_n}^i = \theta_{d_{n-1}}^i - l_{in} \nabla \mathcal{L}_{sup}^i$ 
11:       $\theta_{g_n}^i = \theta_{g_{n-1}}^i - l_{in} \nabla \mathcal{L}_{sup}^i$ 
12:      Compute  $\mathcal{L}_{qry}^{i,n}$  on  $\mathcal{T}_{qry}^i$  via Eq. (11)
13:    End
14:     $\mathcal{L}_{qry}^i = \mathcal{L}_{qry}^{i,\eta}$ 
15:  End
16:  Update  $\theta_s \leftarrow \theta_s - l_{out} \nabla \theta_s \frac{1}{M} \sum_{i=1}^M \mathcal{L}_{qry}^i$ 
17:  Update  $\theta_v \leftarrow \theta_v - l_{out} \nabla \theta_v \frac{1}{M} \sum_{i=1}^M \mathcal{L}_{qry}^i$ 
18:  Update  $\theta_d \leftarrow \theta_d - l_{out} \nabla \theta_d \frac{1}{M} \sum_{i=1}^M \mathcal{L}_{qry}^i$ 
19: End while

```

---

**Algorithm 3 MLDGG W/O RL (Ablation Study 2)**


---

```

1: While not done do:
2:   For each task  $\mathcal{T}^i$  do:
3:      $R_0^i = X^i$ 
4:     Compute  $F^i$  using Eq. (3)
5:     Sample  $H$  times over  $F^i$  to obtain  $A^i$ 
6:     Compute  $R^i$  using Eq. (7)
7:      $\theta_{t_0}^i = \theta_t, \theta_{g_0}^i = \theta_g$ 
8:     Sample  $\mathcal{T}_{qry}^i$  and  $\mathcal{T}_{sup}^i$ 
9:     For  $n$  in  $1, \dots, \eta$  do:
10:      Compute  $\mathcal{L}_{sup}^i$  on  $\mathcal{T}_{sup}^i$  via Eq. (11)
11:       $\theta_{t_n}^i = \theta_{t_{n-1}}^i - l_{in} \nabla \mathcal{L}_{sup}^i$ 
12:       $\theta_{g_n}^i = \theta_{g_{n-1}}^i - l_{in} \nabla \mathcal{L}_{sup}^i$ 
13:      Compute  $\mathcal{L}_{qry}^{i,n}$  on  $\mathcal{T}_{qry}^i$  via Eq. (11)
14:    End
15:     $\mathcal{L}_{qry}^i = \mathcal{L}_{qry}^{i,\eta}$ 
16:  End
17:  Update  $\theta_t \leftarrow \theta_t - l_{out} \nabla \theta_t \frac{1}{M} \sum_{i=1}^M \mathcal{L}_{qry}^i$ 
18: End while

```

---

$$\begin{aligned}
\epsilon_{\text{Acc}}^{e_T}(\hat{f} \circ g) &\leq \frac{1}{K} \sum_{i=1}^K \epsilon_{\text{Acc}}^{e_i}(\hat{f} \circ g) + \frac{\sqrt{2}\pi_u}{K} \sum_{i=1}^K d_{JS}(\mathbb{P}_{S,Y}^{e_T}, \mathbb{P}_{S,Y}^{e_i}) \\
&\stackrel{(1)}{\leq} \frac{1}{K} \sum_{i=1}^K \epsilon_{\text{Acc}}^{e_i}(\hat{f} \circ g) + \frac{\sqrt{2}\pi_u}{K} \sum_{i=1}^K d_{JS}(\mathbb{P}_{S,Y}^{e_T}, \mathbb{P}_{S,Y}^{e_*}) \\
&\quad + \frac{\sqrt{2}\pi_u}{K} \sum_{i=1}^K d_{JS}(\mathbb{P}_{S,Y}^{e_*}, \mathbb{P}_{S,Y}^{e_i}) \\
&\stackrel{(2)}{\leq} \frac{1}{K} \sum_{i=1}^K \epsilon_{\text{Acc}}^{e_i}(\hat{f} \circ g) + \sqrt{2}\pi_u \min_{i \in [K]} d_{JS}(\mathbb{P}_{S,Y}^{e_T}, \mathbb{P}_{S,Y}^{e_i}) \\
&\quad + \sqrt{2}\pi_u \max_{i,j \in [K]} d_{JS}(\mathbb{P}_{S,Y}^{e_i}, \mathbb{P}_{S,Y}^{e_j})
\end{aligned} \tag{18}$$

**Algorithm 4 MLDGG W/O MAML (Ablation Study 3)**


---

```

1: While not done do:
2:   For each source graphs  $G^i$  do:
3:      $R_0^i = X^i$ 
4:     Compute  $F^i$  using Eq. (3)
5:     Sample  $H$  times over  $F^i$  to obtain  $A^i$ 
6:     Compute  $R^i$  using Eq. (7)
7:      $\theta_{t_0}^i = \theta_t, \theta_{s_0}^i = \theta_s, \theta_{v_0}^i = \theta_v, \theta_{d_0}^i = \theta_d, \theta_{g_0}^i = \theta_g$ 
8:     For  $n$  in  $1, \dots, \eta$  do:
9:       Compute  $\mathcal{L}^i$  via Eq. (11)
10:       $\theta_{t_n}^i = \theta_{t_{n-1}}^i - l_{in} \nabla \mathcal{L}^i$ 
11:       $\theta_{s_n}^i = \theta_{s_{n-1}}^i - l_{in} \nabla \mathcal{L}^i$ 
12:       $\theta_{v_n}^i = \theta_{v_{n-1}}^i - l_{in} \nabla \mathcal{L}^i$ 
13:       $\theta_{d_n}^i = \theta_{d_{n-1}}^i - l_{in} \nabla \mathcal{L}^i$ 
14:       $\theta_{g_n}^i = \theta_{g_{n-1}}^i - l_{in} \nabla \mathcal{L}^i$ 
15:     End
16:   End
17: End while

```

---

**Algorithm 5 MLDGG W/O inner-SL (Ablation Study 4)**


---

```

1: While not done do:
2:   For each task  $\mathcal{T}^i$  do:
3:      $R_0^i = X^i$ 
4:     Compute  $F^i$  using Eq. (3);
5:     Sample  $H$  times over  $F^i$  to obtain  $A^i$ 
6:     Compute  $R^i$  using Eq. (7)
7:      $\theta_{t_0}^i = \theta_t, \theta_{s_0}^i = \theta_s, \theta_{v_0}^i = \theta_v, \theta_{d_0}^i = \theta_d, \theta_{g_0}^i = \theta_g$ 
8:     Sample  $\mathcal{T}_{qry}^i$  and  $\mathcal{T}_{sup}^i$ 
9:     For  $n$  in  $1, \dots, \eta$  do:
10:      Compute  $\mathcal{L}_{sup}^i$  on  $\mathcal{T}_{sup}^i$  via Eq. (11)
11:       $\theta_{s_n}^i = \theta_{s_{n-1}}^i - l_{in} \nabla \mathcal{L}_{sup}^i$ 
12:       $\theta_{v_n}^i = \theta_{v_{n-1}}^i - l_{in} \nabla \mathcal{L}_{sup}^i$ 
13:       $\theta_{d_n}^i = \theta_{d_{n-1}}^i - l_{in} \nabla \mathcal{L}_{sup}^i$ 
14:       $\theta_{g_n}^i = \theta_{g_{n-1}}^i - l_{in} \nabla \mathcal{L}_{sup}^i$ 
15:      Compute  $\mathcal{L}_{qry}^{i,n}$  on  $\mathcal{T}_{qry}^i$  via Eq. (11)
16:     End
17:      $\mathcal{L}_{qry}^i = \mathcal{L}_{qry}^{i,\eta}$ 
18:   End
19:   Update  $\theta_t \leftarrow \theta_t - l_{out} \nabla \theta_t \frac{1}{M} \sum_{i=1}^M \mathcal{L}_{qry}^i$ 
20:   Update  $\theta_s \leftarrow \theta_s - l_{out} \nabla \theta_s \frac{1}{M} \sum_{i=1}^M \mathcal{L}_{qry}^i$ 
21:   Update  $\theta_v \leftarrow \theta_v - l_{out} \nabla \theta_v \frac{1}{M} \sum_{i=1}^M \mathcal{L}_{qry}^i$ 
22:   Update  $\theta_d \leftarrow \theta_d - l_{out} \nabla \theta_d \frac{1}{M} \sum_{i=1}^M \mathcal{L}_{qry}^i$ 
23: End while

```

---

Here we have  $\stackrel{(1)}{\leq}$  by using triangle inequality for JS-distance:  $d_{JS}(\mathbb{P}, \mathbb{Z}) \leq d_{JS}(\mathbb{P}, \mathbb{Q}) + d_{JS}(\mathbb{Q}, \mathbb{P})$  with  $\mathbb{P}, \mathbb{Q}$ , and  $\mathbb{Z} = \mathbb{P}^{e_T}, \mathbb{P}^{e_*}$  and  $\mathbb{P}^{e_i}$ , respectively. The previous work have  $\stackrel{(2)}{\leq}$  because  $e_* \in \{e_i\}_{i=1}^K$  then  $d_{JS}(\mathbb{P}_{S,Y}^{e_*}, \mathbb{P}_{S,Y}^{e_i}) \leq \max_{i,j \in [K]} d_{JS}(\mathbb{P}_{S,Y}^{e_i}, \mathbb{P}_{S,Y}^{e_j})$ . However, upon examination, we believe that using the min symbol for the second term on

**Algorithm 6** MLDGG W/O inner-RL (Ablation Study 5)

---

```

1: While not done do:
2:   For each task  $\mathcal{T}^i$  do:
3:      $R_0^i = X^i$ 
4:     Compute  $F^i$  using Eq. (3)
5:     Sample  $H$  times over  $F^i$  to obtain  $A^i$ 
6:     Compute  $R^i$  using Eq. (7)
7:      $\theta_{t_0}^i = \theta_t, \theta_{s_0}^i = \theta_s, \theta_{v_0}^i = \theta_v, \theta_{d_0}^i = \theta_d, \theta_{g_0}^i = \theta_g$ 
8:     Sample  $\mathcal{T}_{qry}^i$  and  $\mathcal{T}_{sup}^i$ 
9:     For  $n$  in  $1, \dots, \eta$  do:
10:      Compute  $\mathcal{L}_{sup}^i$  on  $\mathcal{T}_{sup}^i$  via Eq. (11)
11:       $\theta_{t_n}^i = \theta_{t_{n-1}}^i - l_{in} \nabla \mathcal{L}_{sup}^i$ 
12:       $\theta_{g_n}^i = \theta_{g_{n-1}}^i - l_{in} \nabla \mathcal{L}_{sup}^i$ 
13:      Compute  $\mathcal{L}_{qry}^{i,n}$  on  $\mathcal{T}_{qry}^i$  via Eq. (11)
14:     End
15:      $\mathcal{L}_{qry}^i = \mathcal{L}_{qry}^{i,\eta}$ 
16:   End
17:   Update  $\theta_t \leftarrow \theta_t - l_{out} \nabla \theta_t \frac{1}{M} \sum_{i=1}^M \mathcal{L}_{qry}^i$ 
18:   Update  $\theta_s \leftarrow \theta_s - l_{out} \nabla \theta_s \frac{1}{M} \sum_{i=1}^M \mathcal{L}_{qry}^i$ 
19:   Update  $\theta_v \leftarrow \theta_v - l_{out} \nabla \theta_v \frac{1}{M} \sum_{i=1}^M \mathcal{L}_{qry}^i$ 
20:   Update  $\theta_d \leftarrow \theta_d - l_{out} \nabla \theta_d \frac{1}{M} \sum_{i=1}^M \mathcal{L}_{qry}^i$ 
21: End while

```

---

the right side of  $\leq^{(2)}$  is not rigorous. Here, we have corrected it to use the max symbol. Therefore, we have

$$\begin{aligned}
\epsilon_{\text{Acc}}^{eT}(\hat{f} \circ g) &\leq \frac{1}{K} \sum_{i=1}^K \epsilon_{\text{Acc}}^{e_i}(\hat{f} \circ g) + \frac{\sqrt{2}\pi_u}{K} \sum_{i=1}^K d_{JS}(\mathbb{P}_{S,Y}^{eT}, \mathbb{P}_{S,Y}^{e_i}) \\
&\leq \frac{1}{N} \sum_{i=1}^K \epsilon_{\text{Acc}}^{e_i}(\hat{f} \circ g) + \sqrt{2}\pi_u \max_{i \in [K]} d_{JS}(\mathbb{P}_{S,Y}^{eT}, \mathbb{P}_{S,Y}^{e_i}) \\
&\quad + \sqrt{2}\pi_u \max_{i,j \in [K]} d_{JS}(\mathbb{P}_{S,Y}^{e_i}, \mathbb{P}_{S,Y}^{e_j}). \tag{19}
\end{aligned}$$

Similarly, we can obtain the upper bound based on the feature space  $\mathcal{A} \times \mathcal{X}$  as follows:

$$\begin{aligned}
\epsilon_{\text{Acc}}^{eT}(\hat{f} \circ g) &\leq \frac{1}{K} \sum_{i=1}^N \epsilon_{\text{Acc}}^{e_i}(\hat{f} \circ g) + \sqrt{2}\pi_u \max_{i \in [K]} d_{JS}(\mathbb{P}_{A,X,Y}^{eT}, \mathbb{P}_{A,X,Y}^{e_i}) \\
&\quad + \sqrt{2}\pi_u \max_{i,j \in [K]} d_{JS}(\mathbb{P}_{A,X,Y}^{e_i}, \mathbb{P}_{A,X,Y}^{e_j}). \tag{20}
\end{aligned}$$

**Lemma 1.** Consider two distributions  $\mathbb{P}_{A,X}^{e_i}$  and  $\mathbb{P}_{A,X}^{e_j}$  over  $\mathcal{A} \times \mathcal{X}$ . Let  $\mathbb{P}_S^{e_i}$  and  $\mathbb{P}_S^{e_j}$  be the induced distributions over  $\mathbb{R}^s$  by mapping function  $g: \mathcal{A} \times \mathcal{X} \rightarrow \mathbb{R}^s$ , then we have:

$$d_{JS}(\mathbb{P}_{A,X}^{e_i}, \mathbb{P}_{A,X}^{e_j}) \geq d_{JS}(\mathbb{P}_S^{e_i}, \mathbb{P}_S^{e_j})$$

**Lemma 2.**  $\forall i, j$ , JS distance between  $\mathbb{P}_{S,Y}^{e_i}$  and  $\mathbb{P}_{S,Y}^{e_j}$  in Eq. (14) can be decomposed:

$$\begin{aligned}
d_{JS}(\mathbb{P}_{S,Y}^{e_i}, \mathbb{P}_{S,Y}^{e_j}) &= d_{JS}(\mathbb{P}_Y^{e_i}, \mathbb{P}_Y^{e_j}) \\
&\quad + \sqrt{2\mathbb{E}_{y \sim \mathbb{P}_Y^{e_i, j}} \left[ d_{JS}(\mathbb{P}_{S|Y}^{e_i}, \mathbb{P}_{S|Y}^{e_j})^2 \right]} \tag{21}
\end{aligned}$$

where  $\mathbb{P}_Y^{e_i, j} = \frac{1}{2}(\mathbb{P}_Y^{e_i} + \mathbb{P}_Y^{e_j})$ .

Based on Lemma 1 and Lemma 2, we can integrate Inequality (19) and Inequality (20) as follows:

$$\begin{aligned} \epsilon_{\text{Acc}}^{e_T}(\hat{f} \circ g) &\leq \underbrace{\frac{1}{K} \sum_{i=1}^K \epsilon_{\text{Acc}}^{e_i}(\hat{f} \circ g)}_{\text{term (i)}} + \underbrace{\sqrt{2\mathbb{E}_{y \sim \mathbb{P}_Y^{e_i, j}} \left[ d_{JS}(\mathbb{P}_{S|Y}^{e_i}, \mathbb{P}_{S|Y}^{e_j})^2 \right]}}_{\text{term (ii)}} \\ &+ \sqrt{2}\pi_c \max_{i \in [K]} d_{JS}(\mathbb{P}_{A, X, Y}^{e_T}, \mathbb{P}_{A, X, Y}^{e_i}) + \sqrt{2}\pi_c \max_{i, j \in [K]} d_{JS}(\mathbb{P}_Y^{e_i}, \mathbb{P}_Y^{e_j}), \end{aligned} \quad (22)$$

and this completes the proof.  $\square$

## E.2 Proof for Theorem 2

*Proof.*

**Lemma 3.** *The following holds for any domain  $e$ :*

$$\sqrt{\epsilon_{\text{Acc}}^e(\hat{f} \circ g)} = \sqrt{\mathbb{E}_e[\mathcal{L}(\hat{f} \circ g(A, X), Y)]} \geq \sqrt{\frac{2\pi_c}{\xi}} d_{JS}(\mathbb{P}_Y^e, \mathbb{P}_{\hat{Y}}^e)^2, \forall \hat{f} \circ g$$

where  $\hat{Y}$  is the prediction made by randomized predictor  $\hat{f} \circ g$ .

Consider a source domain  $e_i$  and target domain  $e_T$ . Because JS-distance  $d_{JS}(\cdot, \cdot)$  is a distance metric, we have triangle inequality:

$$d_{JS}(\mathbb{P}_Y^{e_i}, \mathbb{P}_Y^{e_T}) \leq d_{JS}(\mathbb{P}_Y^{e_i}, \mathbb{P}_{\hat{Y}}^{e_i}) + d_{JS}(\mathbb{P}_{\hat{Y}}^{e_i}, \mathbb{P}_{\hat{Y}}^{e_T}) + d_{JS}(\mathbb{P}_{\hat{Y}}^{e_T}, \mathbb{P}_Y^{e_T})$$

Since  $A, X \xrightarrow{g} S \xrightarrow{\hat{f}} \hat{Y}$ , we have  $d_{JS}(\mathbb{P}_Y^{e_i}, \mathbb{P}_Y^{e_T}) \leq d_{JS}(\mathbb{P}_S^{e_i}, \mathbb{P}_S^{e_T}) \leq (\mathbb{P}_{A, X}^{e_i}, \mathbb{P}_{A, X}^{e_T})$ . Using Lemma 3, the bound holds as follows:

$$\begin{aligned} &\left( d_{JS}(\mathbb{P}_Y^{e_i}, \mathbb{P}_Y^{e_T}) - d_{JS}(\mathbb{P}_X^{e_i}, \mathbb{P}_X^{e_T}) \right)^2 \\ &\leq \left( d_{JS}(\mathbb{P}_Y^{e_i}, \mathbb{P}_{\hat{Y}}^{e_i}) + d_{JS}(\mathbb{P}_{\hat{Y}}^{e_T}, \mathbb{P}_Y^{e_T}) \right)^2 \\ &\leq 2 \left( d_{JS}(\mathbb{P}_Y^{e_i}, \mathbb{P}_{\hat{Y}}^{e_i})^2 + d_{JS}(\mathbb{P}_{\hat{Y}}^{e_T}, \mathbb{P}_Y^{e_T})^2 \right) \\ &\leq \frac{2}{\sqrt{\frac{2\pi_c}{\xi}}} \left( \sqrt{\epsilon_{\text{Acc}}^{e_i}(\hat{f} \circ g)} + \sqrt{\epsilon_{\text{Acc}}^{e_T}(\hat{f} \circ g)} \right) \\ &\leq \sqrt{\frac{4\xi}{\pi_c}} \left( \epsilon_{\text{Acc}}^{e_i}(\hat{f} \circ g) + \epsilon_{\text{Acc}}^{e_T}(\hat{f} \circ g) \right) \end{aligned} \quad (23)$$

The last inequality is AM-GM inequality.

Therefore, we have

$$\epsilon_{\text{Acc}}^{e_i}(\hat{f} \circ g) + \epsilon_{\text{Acc}}^{e_T}(\hat{f} \circ g) \geq \frac{\pi_c}{4\xi} \left( d_{JS}(\mathbb{P}_Y^{e_i}, \mathbb{P}_Y^{e_T}) - d_{JS}(\mathbb{P}_{A, X}^{e_i}, \mathbb{P}_{A, X}^{e_T}) \right)^4$$

. The above holds for any source domain  $e_i$ . Average overall  $K$  source domains, we have

$$\begin{aligned} &\frac{1}{K} \sum_{i=1}^K \epsilon_{\text{Acc}}^{e_i}(\hat{f} \circ g) + \epsilon_{\text{Acc}}^{e_T}(\hat{f} \circ g) \\ &\geq \frac{\pi_c}{4\xi K} \sum_{i=1}^K \left( d_{JS}(\mathbb{P}_Y^{e_i}, \mathbb{P}_Y^{e_T}) - d_{JS}(\mathbb{P}_{A, X}^{e_i}, \mathbb{P}_{A, X}^{e_T}) \right)^4. \end{aligned} \quad (24)$$

$\square$



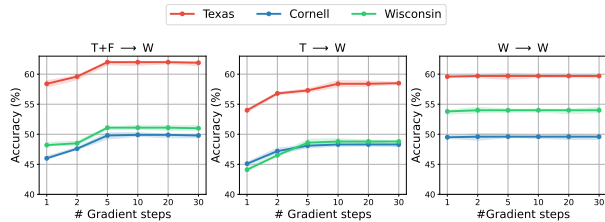
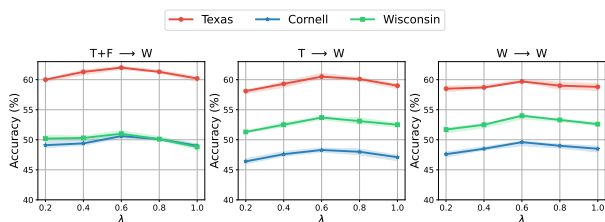


Figure 6: Accuracy with different gradient steps during testing.

Figure 7: Accuracy with different weight of input graph  $\lambda$ .

## F More Experiment Results

### F.1 Sensitivity Analysis.

We evaluate the sensitivity of MLDGG to varying numbers of gradient steps during meta-testing and the weight of the original graph  $\lambda$ . The results are shown in Fig 6 and Fig 7. Owing to space constraints, we report the results for three graphs in WEBKB across the three scenarios. Similar sensitivity trends are observed across other graphs as well. We notice that in-dataset scenarios, fewer update steps are required to attain optimal results compared to cross-dataset scenarios. This is attributed to the greater similarity in semantic information between the test and training domains when sourced from the same dataset. Notably, for cross-dataset scenarios, it can quickly adapt to target graphs with very little fine-tuning, and for in-dataset scenarios, it can achieve good performance even without any fine-tuning. This phenomenon indicates that the meta-learned structure learner and representation learner can be applied to the target graph to achieve high accuracy. Overall, the model is robust to  $\lambda$ . When we use only the input graph as GNN input ( $\lambda = 1$ ), the performance degrades, indicating the importance of the structure learner.